EPFL

NEST | Empa eawag aquatic research

SolAce

Research activities report

Energy use, Daylighting and Indoor comfort

12/09/2019

Pietro Florio
Marta Benedetti
Yujie Wu
Ali Motamed
Xavier Tendon
Jean-Louis Scartezzini

Ecole Polytechnique Fédérale de Lausanne
Laboratoire d'Energie Solaire et de Physique du Bâtiment

This page is intentionally left blank

Contents

Abstract

The SolAce unit at NEST has been designed to meet the highest standards in terms of indoor comfort and energy performance. This report presents a first stage post-occupancy evaluation and an assessment of operational and embodied energy indicators, as well as daylighting and thermal comfort: a brief focus on CO_2 emissions is also included.

Daylighting maximization is among the most evident objectives of SolAce. The unit features an average daylight factor equal to 5%. An effective light redirection from the blinds to the ceiling and the walls in the back of the rooms were observed, contributing to a valuable daylight uniformity.

Space heating needs are proven to be very low, in the order of 28 [kWh/(m^2 year)], while maintaining comfortable thermal conditions throughout 88% of the occupation time in the heating season. Domestic hot water needs, are certainly below 11 [kWh/(m^2 year)], with important fluctuations due to the intermittent use of the shower and the water taps.

If connected to the medium temperature water network (MTE), the solar thermal collectors could comfortably cover both heating and domestic hot water needs, with an annual generation of 46 [kWh/(m^2 year)]: such generation potential doubles the current production injected to the high temperature network (HTE), due to temperature ranges constraints. A system modification in this sense has already been planned.

Electricity needs of about 20 [kWh/(m^2 year)] are almost entirely covered by the photovoltaic modules, which feature an yearly production of 17 [kWh/(m^2 year)]. Overall, the unit operation is already energy positive when considering space heating, domestic hot water and electric appliances needs. With the inclusion of cooling, it is reasonable to expect the energy neutrality of the unit throughout its operational phase.

Embodied energy of the unit is estimated to 39.2 [kWh/(m^2 year)], which is below the limits recommended by the label Minergie-ECO. By considering the carbon sequestration of the wood products during their lifespan, the SolAce unit can be considered also close to the carbon neutrality: the 822 [kg CO_2 / year] emitted by the unit are indeed compensated by 745 [kg CO_2 / year] stored within wood products.

Objective

The goal of this technical report is to compare on-site monitored and computer simulated variables as for daylighting, space-heating, domestic hot water and electrical appliances. A brief focus on embodied energy and CO_2 emissions is also included. In a first stage, this work may also be useful to assess the performance gap between the SolAce unit design and actual operation. Secondly, in case of planned modification scenarios of the building or the energy systems, the effects of the latter can be examined using simulations first, before realization. As such, more informed decisions could be made before proceeding to costly interventions. Among possible modification scenarios, one may include the ones gathered in the following table, associated to specific simulation models.

Modification scenarios	**Analysis type (hourly resolution)**	**Relevant model**
Envelope technologies • New glazing • New cladding • New blinds	• Thermal (useful) energy demand • Approx. Electricity needs • Thermal comfort	EnergyPlus SolaceEnNeeds (see Part II. Space Heating)
	• Daylight Factors (annual resolution)	Simplified Radiance model (see section 3.2)
	• Lighting and daylighting metrics • Visual comfort • Glare risks	EnergyPlus SolaceEnNeeds export to Radiance + necessary radiance materials and adapted simulation parameters
	• Life Cycle Analysis (GWP, NRE, embodied energy)	KBOB (Xavier Tendon) (see Part V)
	• Life Cycle Analysis (human health, environmental impact, biodiversity)	necessary Simapro model
Energy System • New emission terminals (such as radiators, fan coils, etc.), boilers, heat exchangers • New valves, pumps, hydraulic components • New batteries, electric components	• Thermal (final) energy demand • Electricity needs	EnergyPlus SolaceEnNeeds + necessary system model
	• Life Cycle Analysis (any impact)	necessary Simapro model
Energy Management System • New control algorithms • New actuators	• Thermal energy demand • Thermal comfort • Electricity needs	EnergyPlus SolaceEnNeeds + necessary Modelica / Simulink / other code implementations
	• Lighting and daylighting metrics • Visual comfort • Glare risks	EnergyPlus SolaceEnNeeds export to Radiance + necessary radiance materials and adapted simulation parameters
Renewable energy systems • New Photovoltaic modules • New inverter and components • New Solar thermal modules • New tank, expansion vase and components	• PV electricity generation	PVSyst (Nicolas Jolissaint) (see Part IV)
	• Solar thermal generation	Polysun (Xavier Tendon) (see Part III)

This report does not include an analysis of monitored vs simulated cooling energy needs. The former have currently been collected at the end of the cooling season of the first year of operation, and are being checked. The latter must yet be calibrated in accordance with the methodology used for space heating and detailed in this report in section 8. A master student at LESO-PB is currently investigating these aspects.

Part I. Daylighting performance

1 Chromaticity of interior surfaces

The characterization of indoor surfaces is important for future daylighting simulations. Chromaticity is an objective specification of the quality of a color regardless of its luminance. It consists of two independent parameters, often specified as hue (h) and colorfulness (s), where the latter is alternatively called saturation, chroma, intensity, or excitation purity. This number of parameters follows from trichromacy of vision of humans, which is assumed by most models in color science.

The chromaticity of the interior surfaces of SolAce was measured by means of a colorimeter (or "chroma metre") MINOLTA CR-200b. The coordinates Yxy (CIE 1931) were used. Measurements were performed by Pietro Florio and Jérémy Fleury on April 11th, 2019. (Figure 1-1)

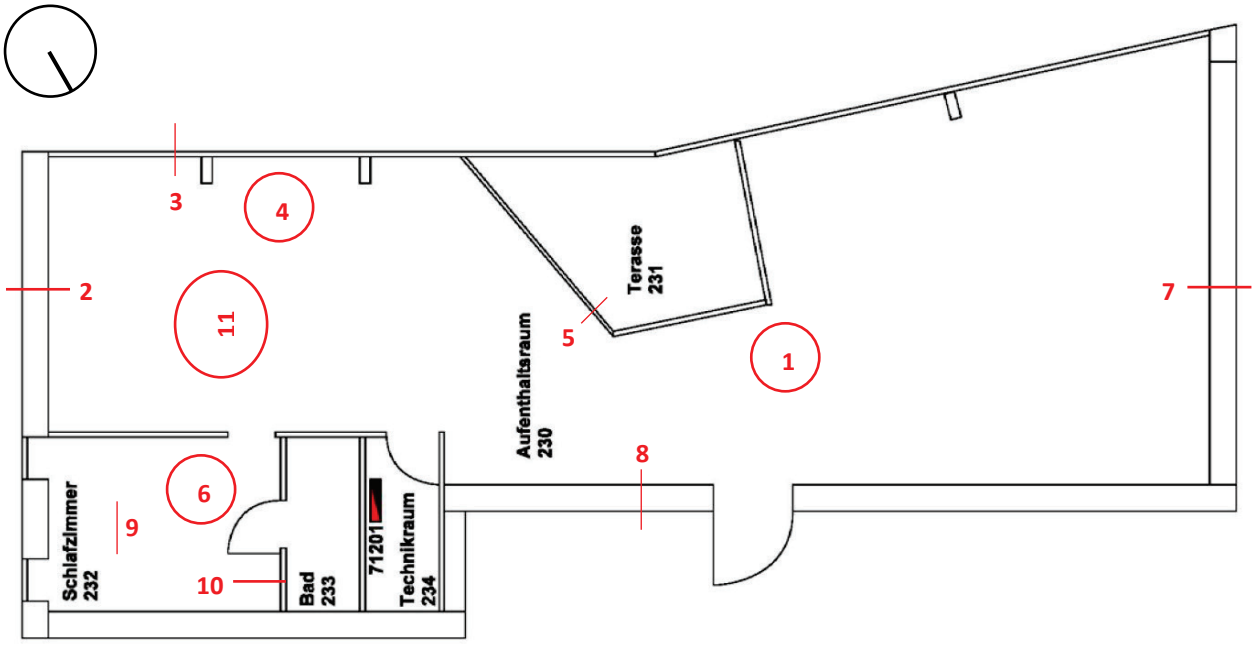

Figure 1-1 : Measurement points in the unit.

2 Results

The results of the measurements are reported in

Table 1.

Point	Description	Y (reflectance) [%]±0.0005	x	y
1	Floor	46	0.317	0.326
2	Wall S-E	71.7	0.316	0.320
3	Window wooden frame	48	0.372	0.364
4	Ceiling	77.6	0.317	0.323
5	Window frame	54.8	0.355	0.350
6	Bedroom floor	17.3	0.433	0.336
7	Wall entrance	76	0.313	0.318
8	Storage cupboard	83	0.315	0.318
9	Bedroom cupboard	52	0.363	0.360
10	Bathroom wall	10.1	0.308	0.308
11	Radiator on ceiling	82.4	0.317	0.395

Table 1. Results of chromaticity measurements.

3 Daylight Factors with open blinds

A daylight factor (DF) [1] is the ratio of the illuminance inside a building to the (outdoor) horizontal illuminance outside the building. It is defined as:

$$DF = \frac{E_i}{E_o} \quad (1)$$

where, E_i [lux] = illuminance due to daylight at a point on the indoors working plane, E_o [lux] = simultaneous outdoor illuminance on a horizontal plane from an unobstructed hemisphere of overcast sky (Equation 1).

3.1 Measured Daylight Factor

In this section, the methodology and the results of the Daylight Factor analysis in the SolAce unit are summarized. The measurements were performed by Marta Benedetti and Ali Motamed on February 1st, 2019, in conditions of overcast sky with the deployed partition curtains in the twin offices section and blinds completely retracted in the whole unit. Internal horizontal illuminance values were measured at the height of 77 cm above the ground level at the points shown in Figure 3-1 by means of a luxmeter Konika Minolta CL-200A. The points designated with *W* are located in proximity of the windows. The outdoor illuminance was measured by the weather station located on the rooftop of the building. The measured values of horizontal illuminance E_h, as well as the ratio between inside and outside values, are reported in Table 2 and Figure 4-1.

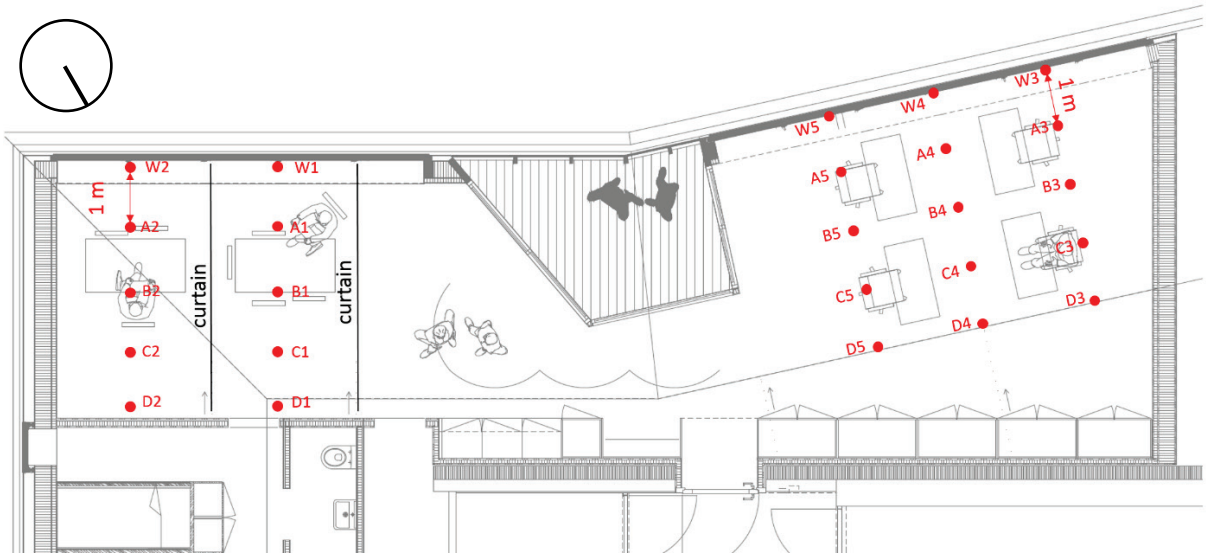

Figure 3-1. Schematic of the measurement points.

		Outside E_h [lux]	Inside E_h [lux]	Ratio (DF)
Living Space	**W1**	10568	1230	12%
	A1	10568	530	5%
	B1	10568	280	3%
	C1	10568	140	1%
	D1	10568	110	1%
Living Space	**W2**	10568	1060	10%
	A2	10568	670	6%
	B2	10568	300	3%
	C2	10568	160	2%

	D2	10568	144	1%
Office	**W3**	7337	1322	18%
	A3	7337	850	12%
	B3	7337	480	7%
	C3	7337	350	5%
	D3	7337	260	4%
Office	**W4**	7337	1340	18%
	A4	7337	850	12%
	B4	7337	700	10%
	C4	7337	530	7%
	D4	7337	450	6%
Office	**W5**	8146	1550	19%
	A5	10568	1100	10%
	B5	10568	650	6%
	C5	10568	410	4%
	D5	10568	320	3%

Table 2. Measured indoor and outdoor horizontal illuminance, and ratio between them Eh.

3.2 Simulated Daylight Factor

Daylight factors were simulated via the Honeybee plugin of the Rhino 3D Grasshopper environment, featuring a Radiance simulation engine. As for the monitoring conditions, partition curtains are deployed, and blinds are completely retracted in the model. The analysis plane is chosen at a relative height of 0.77 m above the floor level; analysis points are sampled on this plane at a resolution of 0.30 m. A standard CIE overcast sky has been used as input, together with standard materials assigned to the walls, the windows and the partitions. These standard materials are available in the default Radiance library (see Table 3), and can be customized with appropriate values for RGB reflectance, specularity and roughness after measured data. However, in the design phase, these values were not defined yet: as such, Radiance standard values are assumed instead, for this reason. Radiance simulation parameters are also listed in the below table.

Surface type	*material type*	*R-G-B Reflectance*	*roughness*	*specularity*
Exterior walls, floor ad ceiling	Plastic	0.5 - 0.5 - 0.5	0	0
Interior walls and partition curtains	Plastic	0.5 - 0.5 - 0.5	0	0

Surface type	*material type*	*R transmissivity*	*G transmissivity*	*B transmissivity*
Windows	Glass	0.654	0.654	0.654

Radiance parameter	*value*
AB ambient bounces	2
AD ambient divisions	1000
AR ambient resolution	300
AD ambient super-samples	128
AA ambient accuracy	0.1

Table 3. Radiance materials and parameters used as simulation input.

Blinds were not integrated in the simulation model at the moment, but may be in the future, by integrating the appropriate BSDF function (see section 6).

Results for simulated daylight factors in the unit are shown in Figure 4-2. On average, the simulated daylighting factor is equal to 4.96%.

4 Results

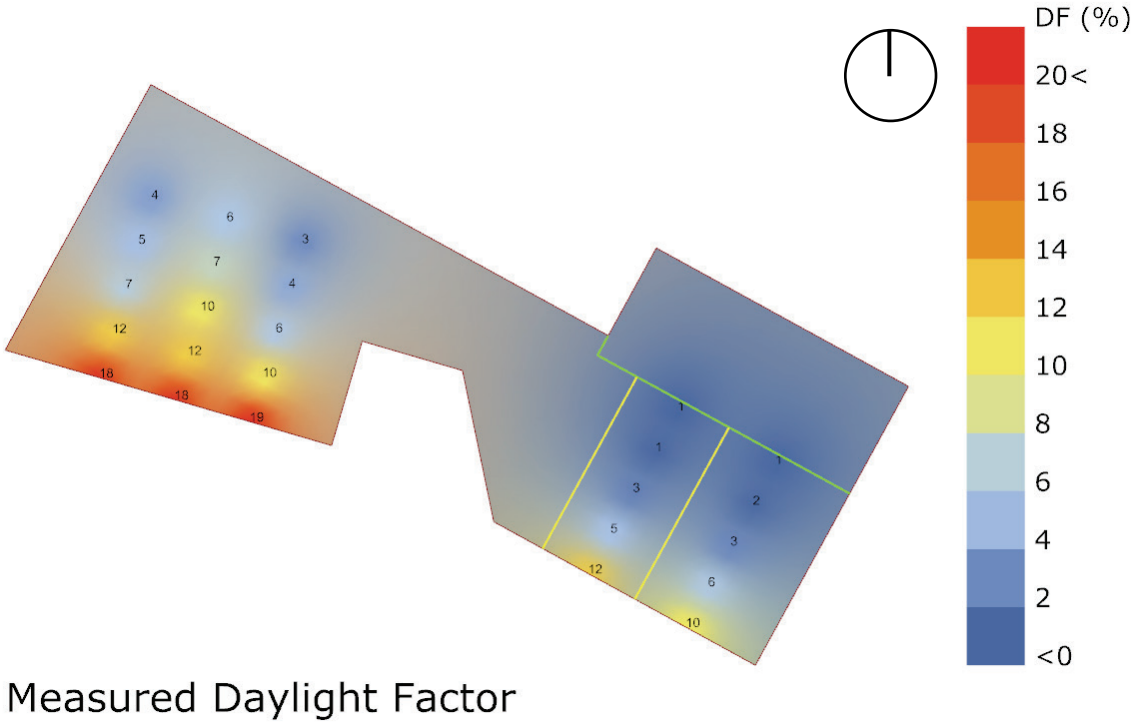

Figure 4-1. Measured daylight factors (DF) [%] at the data points shown in Figure 3-1.

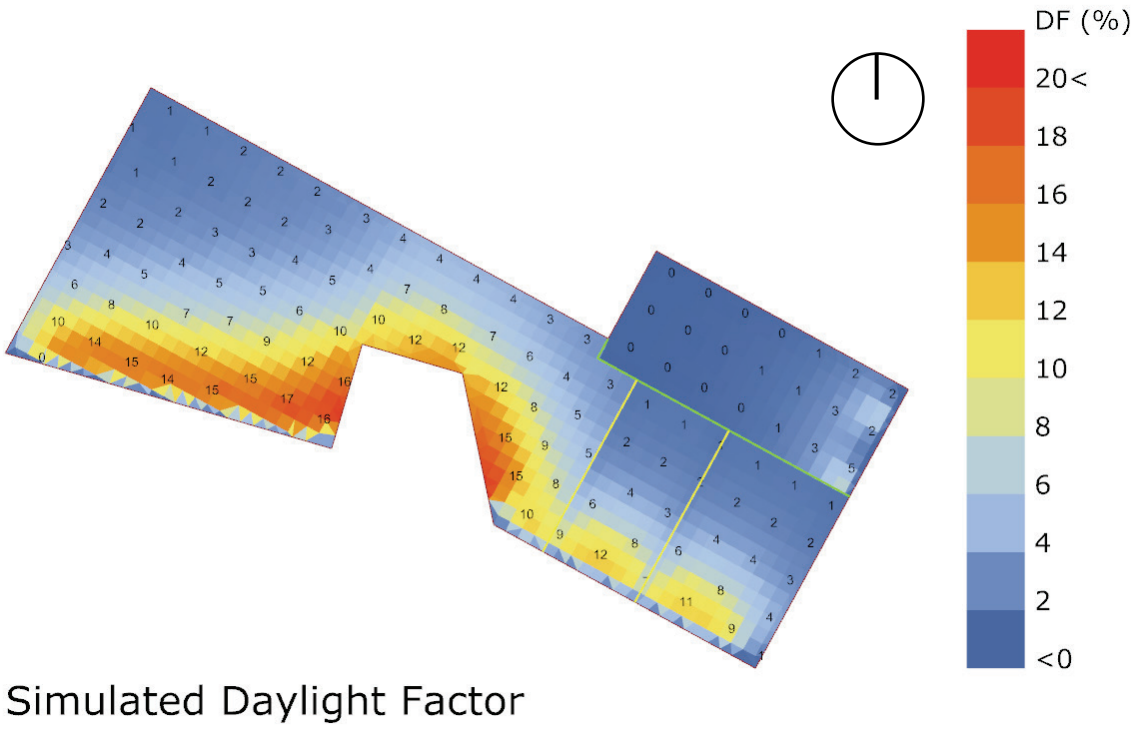

Figure 4-2. Simulated daylight factors (DF) [%] at the resolution of 0.30 m.

The two above maps represent the daylighting factor according to:

1. Measurements taken by Marta Benedetti and Ali Motamed (Figure 4-1)
2. Simulation performed by Pietro Florio (Figure 4-2)

The same color scale is adopted to ease the comparison between the two.

The comparison between the measured data and the simulation of Daylight Factor shows an overall correspondence between the two cases. Even with the default Radiance materials, results show that the range of values is consistent in the two cases.

In the open plan office section, a deeper light penetration is observed in the measured scenario, likely due to higher reflectivity from the ceiling and walls compared to the value set in the simulation. All over the daylighting performance is excellent, showing a high daylighting provision.

Nevertheless, the compliancy of simulated data with monitored values seems to encourage the use of simulation software tools to provide visual comfort insights during the design phase. Further research can be performed by comparing results for annual daylighting metrics to test simulation accuracy in different weather and operational conditions.

5 Illuminance Factors with different blinds states

In this section, we summarize the methodology and results of the daylighting performance assessment of the open office space in the SolAce unit. The monitoring observation was performed by Marta Benedetti and Pietro Florio on June 13th 2019, in clear (to intermediate) sky conditions.

5.1 Measurement points

Indoor horizontal illuminances were measured at the workplane level (about 77cm from the ground) at the locations shown in Figure 5-1. by means of a luxmeter Konika Minolta CL-200A (accuracy $\pm$2%). The glazed doors of the terrace were entirely covered with opaque tissues, in order to block the sunlight coming through, which could represent an additional perturbation in the measurements. The external horizontal illuminance was measured simultaneously on the terrace on the rooftop by means of a luxmeter LMT POCKET LUX 2 (0-200 000 lux, total error $\pm$7%).

5.2 Methodology

The measurements of indoor and outdoor horizontal illuminance were carried out several times. At each set of measurements, the position of the venetian blinds, as well as the slats angle, were varied.

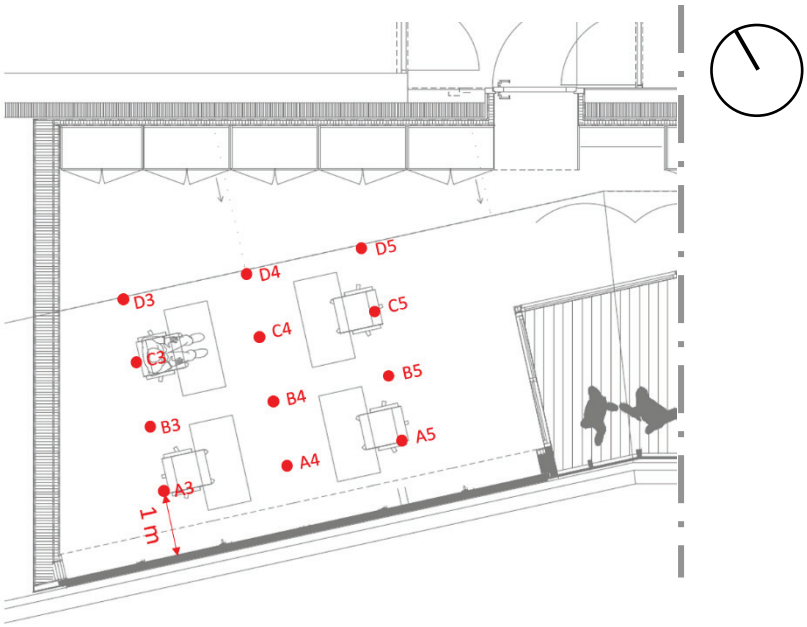

Figure 5-1. Points of measurement of horizontal illuminance in the open plan office.

The measurements were carried out with the following configurations of blinds' position and slat angle (in the bracket we indicate the relative covering fraction in percent and the angle of the slats in degrees). Blinds' position varied between 0 (open), 50% (half open) and 100% (closed); slats angle varied from 0° (horizontal slats), 45° (slats tilted toward indoor) and 90° (vertical slats).

A. Open [0% - 0°]
B. Half, horizontal slats [50% - 0°] (Figure 5-3)
C. Half, tilted [50% - 45°]
D. Half, vertical [50% - 90°] (Figure 5-2)
E. Closed, horizontal [100% - 0°] (Figure 5-4)
F. Closed, tilted [100% - 45°]
G. Closed, vertical [100% - 90°]

Figure 5-3. Half open blinds with horizontal slats (0°).

Figure 5-2. Half open blind with vertical slats (90°).

Figure 5-4. Closed blinds (100%) with horizontal slats (0°).

5.3 Results

The results of the measurements as well as the calculated averages are all reported in Figure 5-5, as well as in the table below.

Half (50%-0°) and fully closed (100%-0°) blinds with horizontal slats show daylight performance close to fully open windows under clear sky, especially in the deepest part of the room. Fully closed (100%-0°) blinds with horizontal slats are even performing better than half closed (50%-0°) indicating a possible daylight deviation on the ceiling.

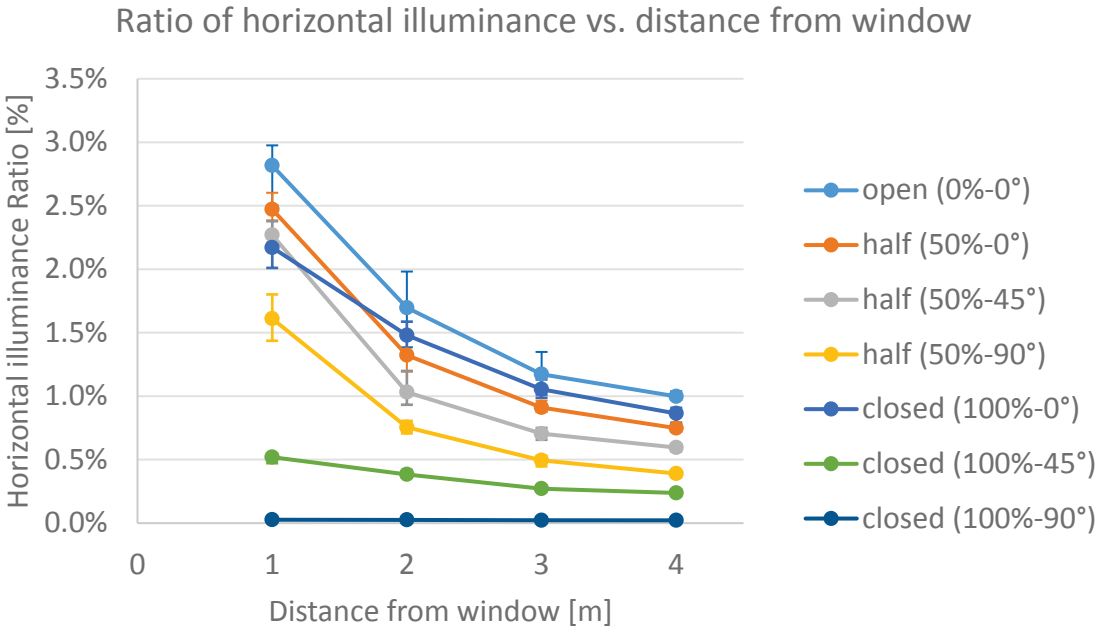

Figure 5-5. Illuminance ratio (= workplane illuminance measured at a location in the office / outdoor horizontal illuminance) vs. distance from the window.

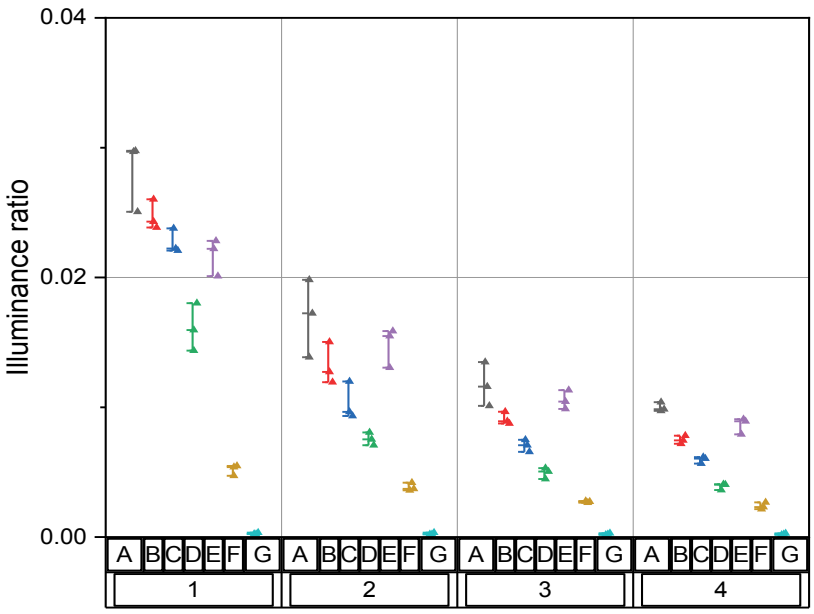

Figure 5-6. Boxplot: another representation of the results. The x-axis represents the distance from the window.

blinds state	timestamp start (CEST)	outside illum. Start (lux)	A3	B3	C3	D3	A4	B4	C4	D4	A5	B5	C5	D5	outside illum end (lux)	timestamp end (CEST)	outside lux average	Average A	Average B	Average C	Average D	Ratio A	RatioB	RatioC	RatioD
open (0%-0°)	13.00	115700	3507	2341	1593	1148	3515	2036	1369	1163	2960	1636	1194	1227	120560		118130.00	3327	2004	1385	1179	2.82%	1.70%	1.17%	1.00%
half (50%-0°)	13.23	124380	3203	1850	1188	884	2991	1566	1098	917	2935	1469	1077	961	121790		123085.00	3043	1628	1121	921	2.47%	1.32%	0.91%	0.75%
half (50%-45°)	13.30	119030	2839	1431	895	675	2654	1151	844	735	2634	1113	784	722	119700	13.33	119365.00	2709	1232	841	711	2.27%	1.03%	0.70%	0.60%
half (50%-90°)	13.42	118690	1865	942	621	423	2107	880	591	475	1680	827	523	473	115220	13.45	116955.00	1884	883	578	457	1.61%	0.75%	0.49%	0.39%
closed (100%-0°)	13.49	114040	2519	1756	1183	897	2588	1800	1284	1030	2280	1480	1120	1012	112800	13.52	113420.00	2462	1679	1196	980	2.17%	1.48%	1.05%	0.86%
closed (100%-45°)	14.00	113200	535	408	314	244	610	475	300	262	621	420	309	302	113370	14.04	113285.00	589	434	308	269	0.52%	0.38%	0.27%	0.24%
closed (100%-90°)	14.05	113040	27	24	19	19	26	24	24	24	38	39	34	32	113690	14.08	113365.00	30	29	26	25	0.03%	0.03%	0.02%	0.02%

Table 4. Measured outside and inside horizontal illuminance, and respective illuminance ratios for the different data points.

6 Blinds complex daylight properties

BSDF (Bidirectional Scattering Distribution Function) usually designates the general mathematical function, which describes the way in which the light is scattered by a surface. However, in practice this phenomenon is usually split into the reflected and transmitted components, which are then treated separately as BRDF (Bidirectional Reflectance Distribution Function) and BTDF (Bidirectional Transmittance Distribution Function), see Figure 6-1.

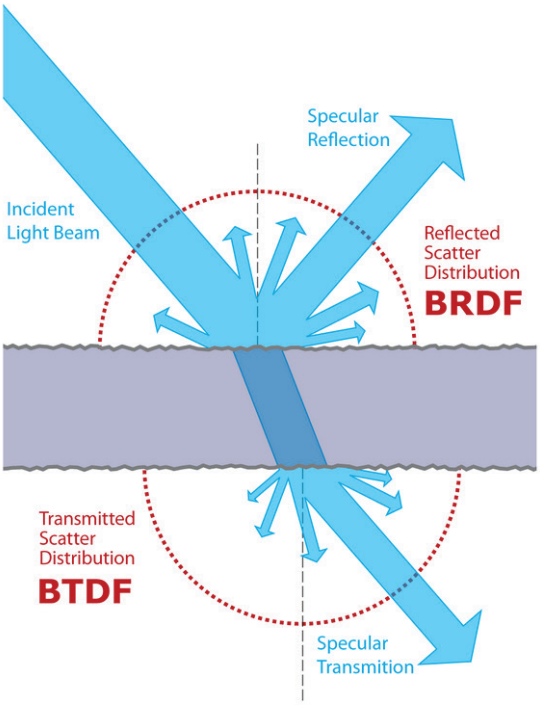

Figure 6-1. Schematic principle of BSDF components. (Image credits: Jurohi on Wikimedia Commons CC)

The Bidirectional Transmittance Distribution Function (BTDF) is a model that comprehensively describes the directional light transmittance property of a certain type of transparent material or a complex fenestration system. Goniophotometers and computational tools have been developed to monitor and simulate the BTDF of a complex fenestration system respectively.

BTDF is defined by the ratio of emergent radiance L to incident irradiance E on the incident plane, as described in Equation 2 [2], where the subscript i denotes an incident direction, t refers to a transmitted direction, and θ and ϕ are the zenith angle and azimuth angle in spherical coordinates, respectively. The function is generally specified with wavelength λ when a spectral dependent property is considered and is assumed to have spatial uniformity on the incident plane. In the context of photometric quantities, BTDF can be integrated with the photopic luminosity function V(λ) over the wavelength λ to eliminate the dimension.

$$f(\theta_i, \varphi_i; \theta_t, \varphi_t; \lambda) = \frac{L_t(\theta_i,\varphi_i;\theta_t,\varphi_t;\lambda)}{E_i(\theta_i,\varphi_i;\lambda)} \quad (2)$$

A small sample of Grinotex III slats were fitted with a frame and fixed on the goniophotometer in EPFL to quantify the BTDF data regarding the light transmittance behaviour, as shown in Figure 6-2. Two different tilt angles were selected, including the horizontal (0°) and 45° inclined slats. The incident rays with elevation angle 60° and 24° were chosen to depict the sun position during summer and winter season at noon (90° azimuth angle) in Switzerland, respectively.

Figure 6-2. Grinotex III sample fixed on the Goniophotometer.

Figure 6-3 illustrates the photometric solids of BTDF data with horizontal slats of the Grinotex blinds. With 60° incident elevation angle (summer), majority of the emergent light is re-direct upward (to the ceiling), which helps illuminate deep regions of a room and mitigate discomfort glare for occupants close to facades. With 24° incident elevation angle (winter), the light is transmitted through the slots between slats, potentially mitigate occupants' visual comfort.

Figure 6-4 illustrates the photometric solids of BTDF data with 45° inclined slats of the Grinotex blinds. With 60° incident elevation angle (summer), the daylight is not only re-directed upward (to the ceiling) but also diffused downward (to the work-plane). With 24° incident elevation angle (winter), most of the light is re-directed upward (to the ceiling), which potentially protects occupants from discomfort glare in winter seasons and improve the lighting condition in deep regions of a room.

Such a favorable redirection of the direct sun component (e.g. sunlight) can be observed on Figure 5-3, showing a brighter ceiling close to the window.

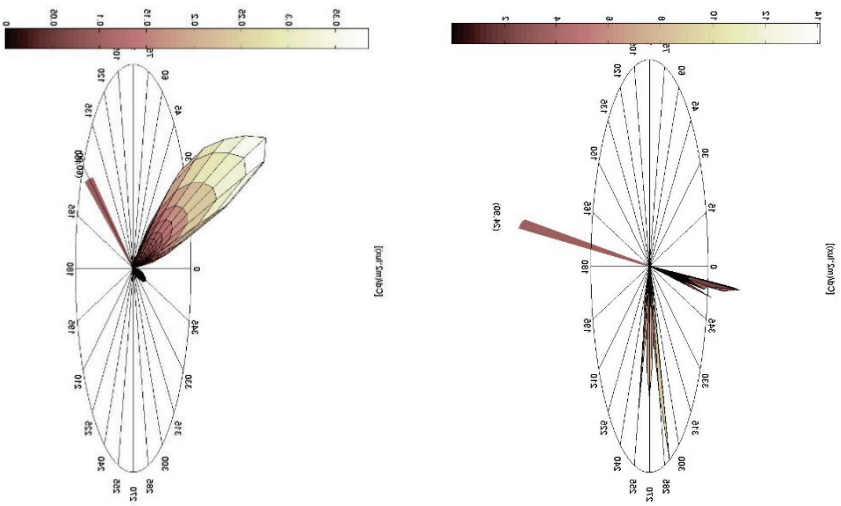

Figure 6-3. Corresponding photometric solids of BTDF data of Grinotex III with horizontal slats a) 60° incident elevation angle b) 24° incident elevation angle.

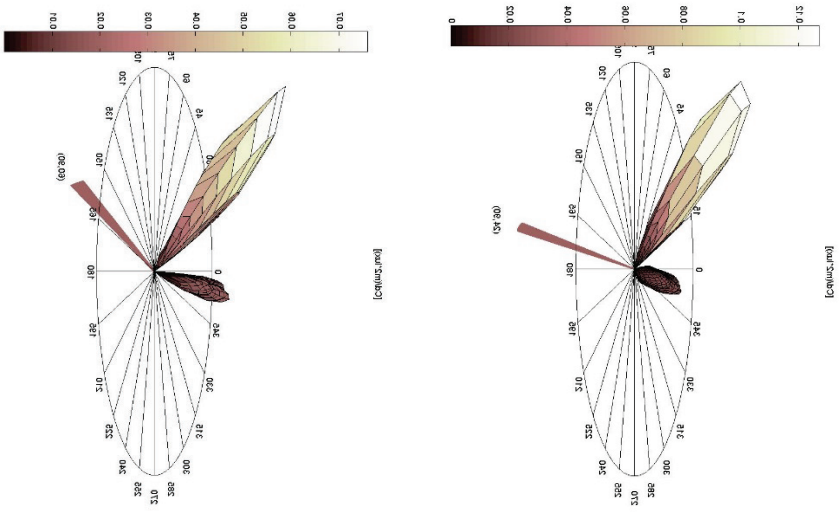

Figure 6-4. Corresponding photometric solids of BTDF data of Grinotex III with 45° inclined slats a) 60° incident elevation angle b) 24° incident elevation angle.

Part II. Space heating

7 Space heating simulation

The methodology of the simulation relies on different software tools, with a specific purpose each:

1. **Rhinoceros** is a popular 3D computer graphics and computer-aided design (CAD) application, which manipulates freeform surfaces, mathematically modeled surfaces (NURBS) and meshes. Building geometry can be easily modelled in Rhino and imported from major building information modeling (BIM) and CAD software.
2. **Grasshopper** is a module that permits the parametric interaction with objects modeled in Rhinoceros, as well as their modification through visual programming and extraction of their attributes.
3. **Ladybug tools** is a set of Python and Grasshopper code blocks allowing the model implementation with ray-tracing algorithms (Radiance) and building energy modeling software (EnergyPlus) [3].
4. **Open Studio** is a tool that contains useful libraries of schedules, HVAC system components and other elements needed to perform building energy simulations in EnergyPlus [4]. It also provides a graphical user interface to EnergyPlus.
5. **EnergyPlus** is a validated software for dynamic building energy models [5]. It is based on conductive heat transfer and storage equations (CTF). The employed version of EnergyPlus is 8.9.0.
6. **Radiance** is a backwards raytracing software validated for physically reliable lighting simulations [6].

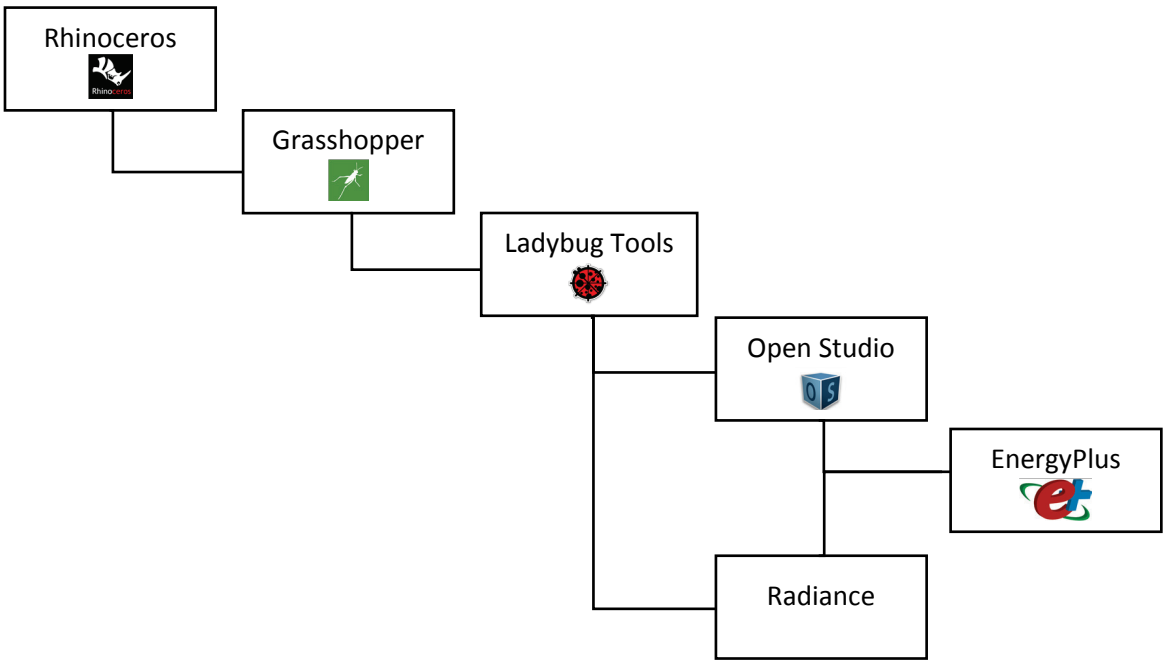

Occasionally, the software illustrated above is complemented by custom Python code, especially at the interfaces and for the results visualization part. The original simulations were carried out by Pietro Florio. A significant contribution to this paragraph is due to Xavier Tendon based on his MSc. Environment thesis [7].

7.1 Zoning and boundary conditions

The SolAce unit is modeled as a single conditioned thermal zone. Only elements comprised within the SolAce unit envelope are considered (i.e. concrete slabs are not taken into account). The following boundary conditions are assumed: all façades are exposed to the outdoors; walls against other units and the central building core are considered as adiabatic (no thermal flux goes through them). The ceiling is considered as exposed to the outdoors, since there is currently no heated unit above SolAce. The floor is assumed as exposed to a space at a constant temperature of 12 °C: this choice is justified by the presence of a heated unit in correspondence of most of the SolAce floor, separated by a 45 cm concrete slab that stores part of the dispersed heat from the two units.

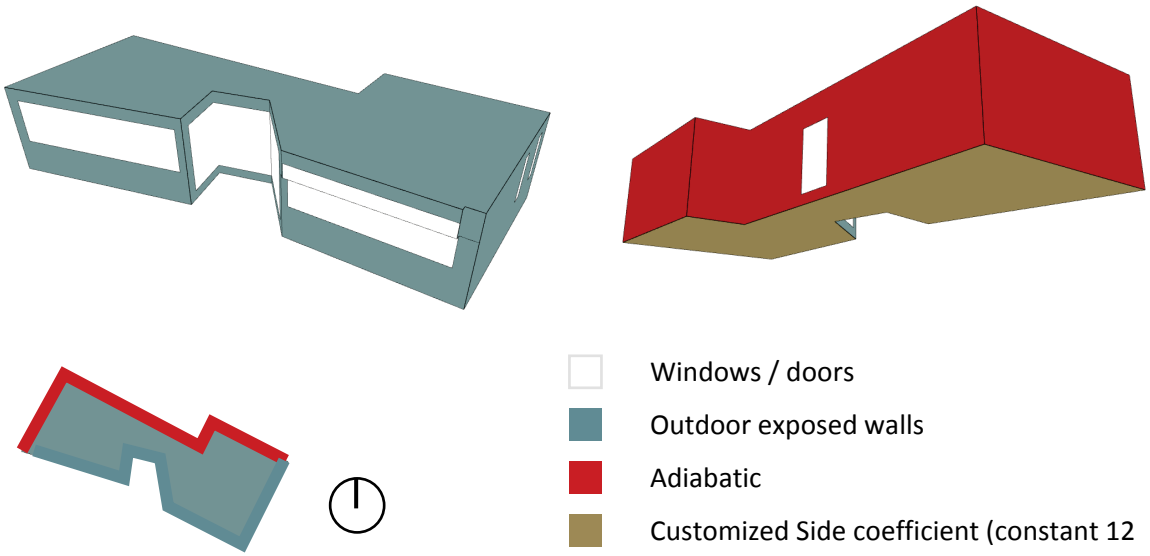

Figure 7-1: Boundary conditions of envelope elements

Shape indicator	Symbol	Value
Envelope surface / gross conditioned volume	S/V	0.28 [-]
Envelope surface / heated floor area	Ath/Ae	0.88 [-]
Heated Floor Area	Ae	94.3 [m^2]
Net conditioned volume	V net	237.8 [m^3]
Gross conditioned vulume	V l	297.2 [m^3]

7.2 Envelope

7.2.1 Opaque elements

Construction details of all envelope elements have been extracted from construction documents. In particular, many characteristics are issued from the psychrometric report of Prof. C.A. Roulet, and updated to the last construction variant by Xavier Tendon. Worth to note is the fact that U-values are averaged to include thermal bridges generated by the wooden beams of the construction panes interrupting the continuity of the insulation, which generate an anisotropic conductivity. The retained U-values are listed in the table below. As stated before, concrete slabs are not included in the construction elements.

Envelope element	U-value [W/m^2 K]	Internal specific heat capacity k1 [kJ/m^2 K]
Exterior wall	0.17	29
Interior wall	0.18	29
Floor	0.19	61

Ceiling	0.22	44

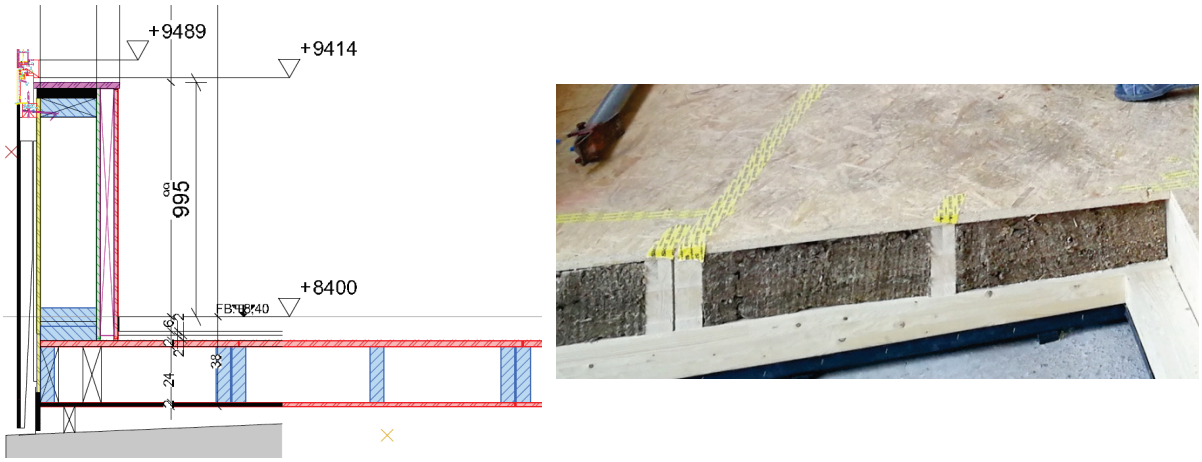

Figure 7-2: Construction detail. On the left the carpentry plan: In blue, the wooden beams that interrupt the insulation continuity. On the right, the photo from the construction site.

7.2.2 Glazing

Windows' U-values for glazing and frame were retrieved from the manufacturer's datasheets and applied to an Energy Plus "Simple Glazing System". The solar heat gain coefficient and the visual transmittance were issued from a standard triple glazing available in the LESOSAI software library. This assumption does not affect thermal calculations significantly, but it may have an impact on daylighting assessment.

Window properties	**Value**
Glazing U-value	0.5 [W/m^2 K]
Frame U-value	1.52 [W/m^2 K]
Solar Heat Gain Coefficient (g-value)	0.59 [-]
Visual transmissivity (tau-value)	0.72 [-]

The above-mentioned values are assumed for all type of glazing, including standard, laser-hatched and "Coolshade" glazing. Given the seasonal variation of the solar heat gain coefficient of the "Coolshade" device, it would be recommended to model the latter as an Energy Plus "Complex Fenestration System": this was not possible at this stage due to the lack of technical data. As such, less solar gains will enter in the SolAce unit in reality compared to this simulation scenario.

7.2.3 Blinds

Blinds and shades details were retrieved from the manufacturer's datasheets. Venetian blinds have been modeled through the Energy Plus "window material blinds" object, while roller blinds are entered as Energy Plus "window material shade" objects. Most important properties are recapitulated in the following table. Details concerning blinds operation are provided in the next section.

Shade properties	**GRIESSER MONTANA SCREEN**
Solar Transmittance	0.11 [-]
Solar Reflectance	0.37 [-]
Visible Transmittance	0.11 [-]
Visible Reflectance	0.37 [-]
Infrared Hemispherical Emissivity	0.9 [-]
Infrared Transmittance	0 [-]
Thickness	0.5 [mm]
Conductivity	221 [W/m K]

Shade to Glass Distance	8.96 [cm]

Blinds properties	**GRIESSER GRINOTEX 3 SINUS**
Slat Orientation	Horizontal
Slat Width	8.5 [cm]
Slat Separation	8.5 [cm]
Slat Thickness	0.5 [mm]
Slat Angle (between slat plane normal and glass plane normal)	65 [deg]
Slat Conductivity	221 [W/m K]
Slat Solar Transmittance (beam and diffuse)	0 [-]
Slat Solar Reflectance, front and back sides (beam and diffuse)	0.55 [-]
Slat Visible Transmittance (beam and diffuse)	0 [-]
Slat Visible Reflectance, front and back sides (beam and diffuse)	0.55 [-]
Slat Infrared Hemispherical Transmittance	0 [-]
Slat Infrared Hemispherical Emissivity, front and back sides	0.9 [-]
Blind to Glass Distance	6.5 [cm]
Minimum Slat Angle	0 [deg]
Maximum Slat Angle	180 [deg]

7.3 Operation

7.3.1 People occupancy

The maximal number of occupants at peak time is three, i.e. circa 0.03 persons/m^2: the generated heat gain is equal to 120 W/person. The occupancy fractions are issued from the NREL OpenStudio default library "Medium Office Bldg Occ": they are shown in Figure 7-3.

On Saturdays between 1st April and 31st December, the fractional profile ranges from 0 to 0.5 with peak time at 14.00 (while it is equivalent to the other weekdays between 1st January and 31st March); on Sundays, the fractional profile is set constant at 0. Public holidays between Monday and Friday are treated as usual workdays.

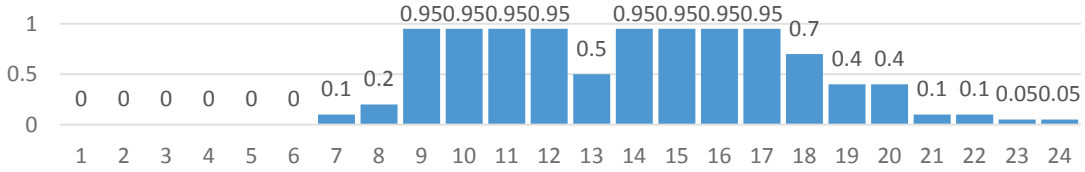

Figure 7-3 : Occupancy fractions on a typical day

7.3.2 Artificial lighting

The lighting power density is equal to 9 W/m^2 at the peak load (when all light sources are on at full power). This value has been calculated by summing up the absorbed electric power of each lighting appliance according to the lighting supplier's documentation (Regent), then dividing this amount by the Heated Floor Area (Ae).

Artificial lighting follows the load profile expressed in Figure 7-5, issued from the NREL OpenStudio default library "Office Bldg Light". On Saturdays between 1st April and 31st December, the fractional profile ranges from 0.05 to 0.5 with peak time at 14.00 (while it is equivalent to the other weekdays between 1st January and 31st March); on Sundays, the fractional profile is set constant at 0.05. Public holidays between Monday and Friday are treated as usual workdays. A continuous dimming occurs whenever the illuminance set point of 500 lux is met at the height of 80 cm above the floor level in the center of the open space office section (Figure 7-4).

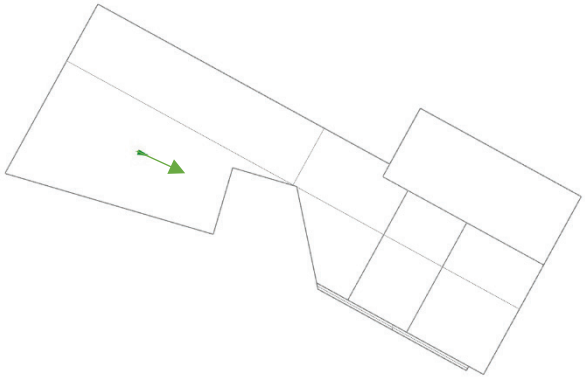

Figure 7-4: Daylighting control point and viewing direction

7.3.3 Electric appliance

Electric appliance power density is equal to 1.6 W/m^2 at the peak load (when all appliances are on). This corresponds to a maximal power of circa 150 W for the whole unit, i.e. the absorbed power of two computer workstations. This choice is justified by the sporadic electricity use in the unit: another option would be to calculate the absorbed power of all appliances installed in the unit and couple it with very low custom load profiles.

Appliances follow the load profile given in Figure 7-5, issued from the NREL OpenStudio default library "Medium Office Bldg Equipment". On Saturdays between 1st April and 31st December, the fractional profile ranges from 0.3 to 0.5 with peak time at 14.00 (while it is equivalent to the other weekdays between 1st January and 31st March); on Sundays, the fractional profile is set constant at 0.3. Public holidays between Monday and Friday are treated as usual workdays.

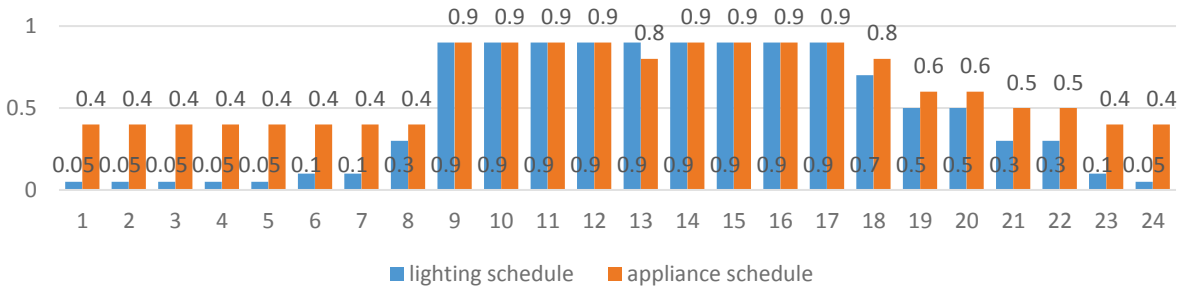

Figure 7-5: Lighting and electric appliances fractional use daily schedule.

7.3.4 Air infiltration

The maximal infiltration flow rate is set to 14.6 [m^3/h], which correspond to an airtight building according to the EN ISO 13790 compliant calculation performed in LESOSAI. This value is equivalent to 0.15 [m^3/h m^2 (AE)], or 0.06 [ACH].

Infiltration rate is multiplied by the following fractional profile: 0.25 between 6.00 and 22.00, 1.00 during the rest of the day as for weekdays: on Saturdays, the value of 0.25 is set between 6.00 and 18.00 only; on Sundays, the infiltration rate constantly multiplies a factor 1.

7.3.5 Natural Ventilation

In the SolAce unit, both natural and mechanical ventilation are foreseen. Natural ventilation is calculated with a simple wind speed and stack effect model (EnergyPlus Zone Ventilation: Wind and Stack Open Area). Windows opening follows the schedule indicated in Figure 7-6, all the year long, including holidays and weekends. Based on the openable windows distribution, it is assumed that 43% of total glazed area can be opened across the entire window height to let fresh air enter the unit.

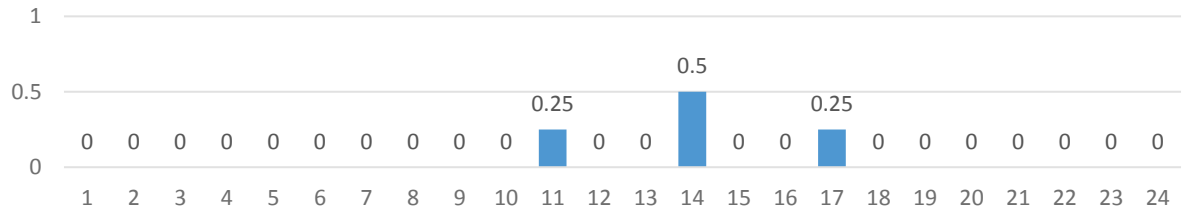

Figure 7-6: Natural ventilation daily operational schedule.

At the scheduled times, windows are only opened whenever the temperature conditions indicated in the following table are met. Windows opening is inhibited whenever wind speed goes beyond 40 [m/s].

Temperature conditions triggering Natural ventilation [°C]				
Min indoor	Max indoor	Min outdoor	Max outdoor	Min delta in-out
23	28	0	26	5

7.3.6 Mechanical Ventilation

The total airflow injected in the unit is the sum of two specific airflows. The first is a specific airflow per conditioned area unit, which ranges from a minimum of 0.43 [m^3/h m^2 (Ae)] to a maximum of 1.91 [m^3/h m^2 (Ae)]: the maximum value has been set according to the technical plans provided by the HVAC engineers.

Mechanical ventilation features				
Min Specific airflow per area	0.00012 [m^3/s m^2 (Ae)]	0.43 [m^3/h m^2 (Ae)]	0.17 [ACH]	40 [m^3/h]
Min Specific airflow per person	0.0001 [m^3/s m^2 (Ae)]	0.36 [m^3/h m^2 (Ae)]	0.14 [ACH]	34 [m^3/h]
Max airflow supported by the system	0.00053 [m^3/s m^2 (Ae)]	1.91 [m^3/h m^2 (Ae)]	0.76 [ACH]	180 [m^3/h]

7.3.7 Blinds operation

A daylighting comfort controller is used for blinds operation: no thermal comfort control is implemented in the current version of the model. As for the daylighting control, a Daylighting Glare Index (DGI) set point is set to 22, at the control point located at the relative height of 120 cm above the floor level in the center of the open space office section, with a view facing the terrace (Figure 7-4). Whenever the DGI is higher, blinds are entirely deployed. The blinds angle is constantly 25 degrees downwards from the horizontal axis. This assumption has both impact on solar gains and on daylighting comfort, thus it has to be treated with care.

7.4 Heating System

The heating system is modeled as an EnergyPlus “Ideal Air Load System”, which supplies air at the desired set point with an ideal efficiency of 100%. This component can be thought of as an ideal unit that mixes zone air with the specified amount of outdoor air and then adds or removes heat and moisture with 100% efficiency in order to meet the specified controls. In practice, the energy input to the ideal air load system corresponds to the spatial heating energy needs, i.e. the useful energy. As such, no real heating system with specific generation, distribution, emission and regulation efficiencies was modeled as for now.

The maximal heating power of the system is set to 4100 [W], which corresponds to the system sizing retrieved in the technical documents of the system engineering company. The heating set point is constantly set to 22 °C, as observed by monitoring, to meet sufficient thermal comfort in the unit at any time. However, heating activation is triggered by specific outdoor air conditions: heating is allowed for a 24h average outdoor air temperature below 11 °C. It is then deactivated for a 24h average outdoor air temperature above 12 °C (dead-band 1 °C).

Heating control temperatures [°C]			
Set point	Set back	Avg. daily outdoor temp. trigger on (D90)	Avg. daily outdoor temp. trigger off (D90+D92)
22	-	<11	>12

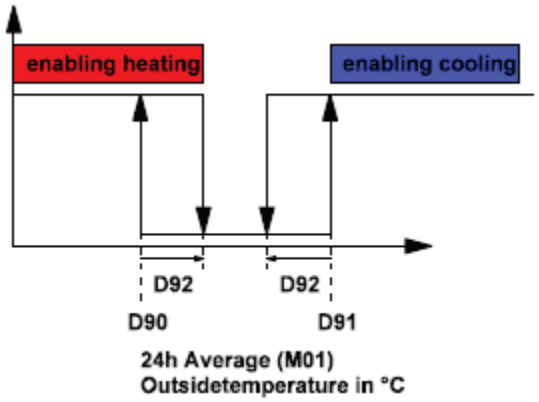

Figure 7-7: heating and cooling control based on outdoor air temperature.

The heating system of the unit features also a temperature control on the hot water mix flowing in the radiative ceiling, i.e. the hot water mix in the heating pipelines decreases in temperature with the increasing outdoor air temperature. However, since the heating system is not modeled here, this temperature control was not considered at that stage.

7.5 Weather data

Weather data for the city of Dübendorf has been generated by interpolation in the Meteonorm software tool. The annual meteorological file includes outdoor air temperature, humidity, solar radiation, wind speed, and other variables at an hourly time step resolution. Generated data reflects a Test Reference Year (TRY), which correspond to an ideal period constituted from the average of the latest decades. In this specific case, temperature data belong to the historical series 1991-2009 and solar radiation data to the historical series 2001-2009. As such, a correspondence with monitored data is not guaranteed, but average weather conditions allow inferring the overall building performance through a more effective generalization.

7.6 Surrounding buildings

Shading on the surfaces of the unit is produced by the surrounding buildings indicated in Figure 7-8, whose shape has been retrieved from an aerial photograph and from a rough estimation of their height based on the number of floors.

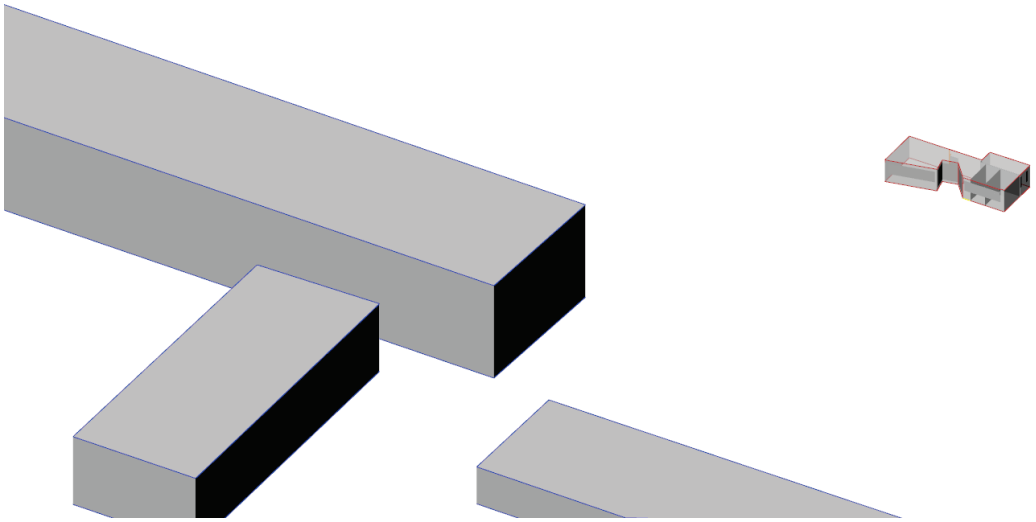

Figure 7-8: Outdoor buildings considered for shading

7.7 Simulation parameters

Shading calculations from the surroundings are updated every 5 days at an hourly time step: this allows to save some computational time by averaging the sun positions per hour over such span, but entails some inaccuracy, especially to the extent of daylight entering the building.

The solar distribution algorithm of the EnergyPlus "Building" class is set to "Full exterior with reflections". In this case, shadow patterns on exterior surfaces caused by detached shading, wings, overhangs, and exterior surfaces of all zones are computed. All beam solar radiation entering the zone is assumed to imping on the floor, where it is absorbed according to the floor's solar absorptance. Any radiation reflected by the floor is added to the transmitted diffuse radiation, which is assumed to be uniformly distributed on all interior surfaces. This assumption is acceptable for thermal energy calculations, but it is not adapted to daylighting calculations and has to be treated with care.

The terrain roughness affecting the wind speed around the building and the external heat losses is set to "Suburbs" in the EnergyPlus "Building" class.

8 Model calibration

Before proceeding to the whole heating season simulation, the model has been calibrated on a single day, representing a typical winter day (21st January). In this case, weather data for the simulation are not extracted from the Test Reference Year, but retrieved from the meteorological station available on top of the NEST building.

Monitored variables and simulated variables can thus be compared on the same basis. After several adjustments that led to the parameters illustrated in the previous section, the results shown in Figure 8-1 and Figure 8-2 could be produced. Simulations on the test day are performed after calculation on a bunch of warm-up days.

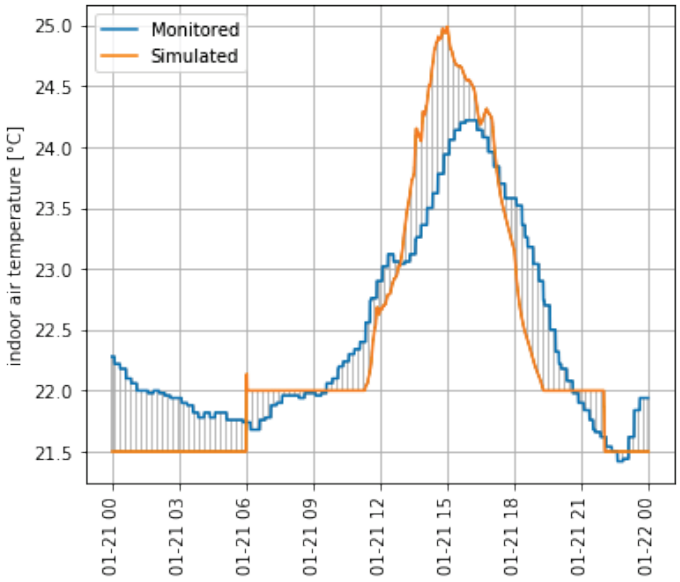

Figure 8-1: Calibration day 21.01: indoor air temperature (simulated against monitored)

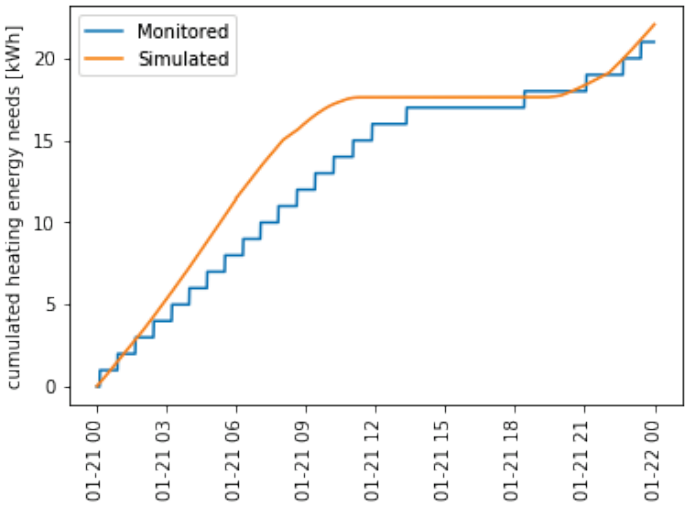

Figure 8-2: Calibration day 21.01: cumulative energy needs (simulated against monitored)

Figure 8-1 shows that there is no significant shift between the simulated indoor air temperature wave and the monitored one at the ceiling level. At maximum, one degree-Celsius difference is observed around the early afternoon at 15.00.

As for the heating energy needs, Figure 8-2 shows that in general, the simulation is a sound approximation of daily energy demand, even though a small divergence in the morning hours expresses a more unfavorable situation in the simulated case.

9 Results

9.1 Global results

After calibration, the model was applied to the whole Test Reference Year. The most significant variables, i.e. indoor air temperature and heating energy needs could be compared against monitored data for the heating season 2018-2019 (22 November 2018, first available day in the monitored database – 22 May 2019). Some discrepancies can be justified by the non-correspondence between real weather data and Test Reference Year data.

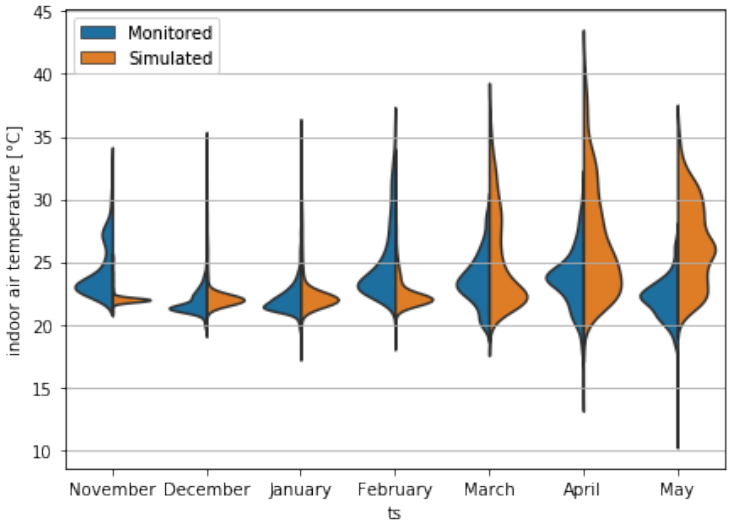

Average temperature difference (monitored vs simulated), absolute value	**2.7 [°C]**

Figure 9-1: Heating season 2018-2019: indoor air temperature (simulated against monitored)

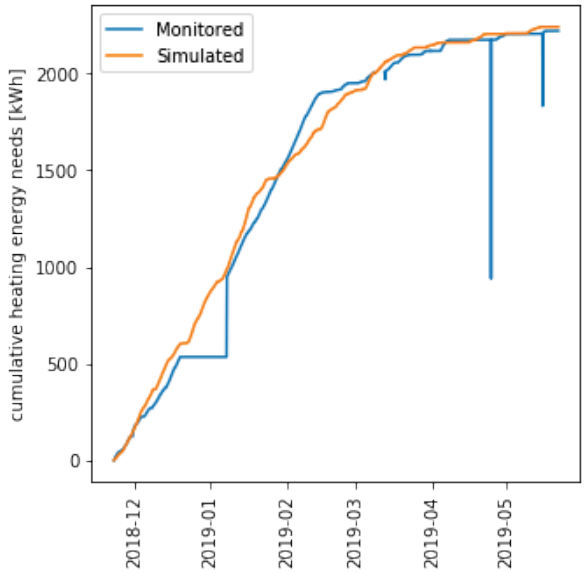

Average difference between heating needs (monitored vs simulated), absolute value	**70 [kWh]**

Figure 9-2: Heating season 2018-2019: cumulative energy needs (simulated against monitored)

Figure 9-1 shows a certain uniformity between simulated and monitored indoor air temperature. The violin plots highlight the correspondence of average monthly temperatures, i.e. the peaks of the distribution curves in the two scenarios (except for May). The simulated scenario features a more focused distribution of temperatures around the average in early winter months: however only 8 days are simulated in November. With the exception of February, a tail towards higher values is observed in simulated temperatures. However, the average difference in temperature between monitored and simulated data equals 2.7 degree-Celsius.

In Figure 9-2, despite some monitoring errors (i.e. missing data and outliers), the trend of the cumulative heating energy needs is reproduced by the simulation quite closely. On average across all hourly time steps in a year, the difference between monitored and simulated heating energy needs is about 70 kWh.

9.2 Hygro-thermal Comfort

The observation of the Fanger's comfort chart represented for simulated data in

Figure 9-3 reveals that the SolAce unit is comfortable for most of the heating season, during occupation time: unoccupied time is neglected in the diagram. Operative temperature has been considered for comfort calculations, to take radiative effects of building components into account. Assuming that office activities are performed by the occupants with adapted clothing levels (0.5 to 1.2 [clo]), 88% of occupation time lies within the comfort conditions. In spite of this, the unit is uncomfortable during several tenths of occupation hours, in which the operative temperature can even go beyond 40 [°C].

To improve comfort results, more effective controls should be implemented in the simulation, for example a thermal comfort control on blinds. This modification could also improve the accuracy of the simulated indoor air temperature.

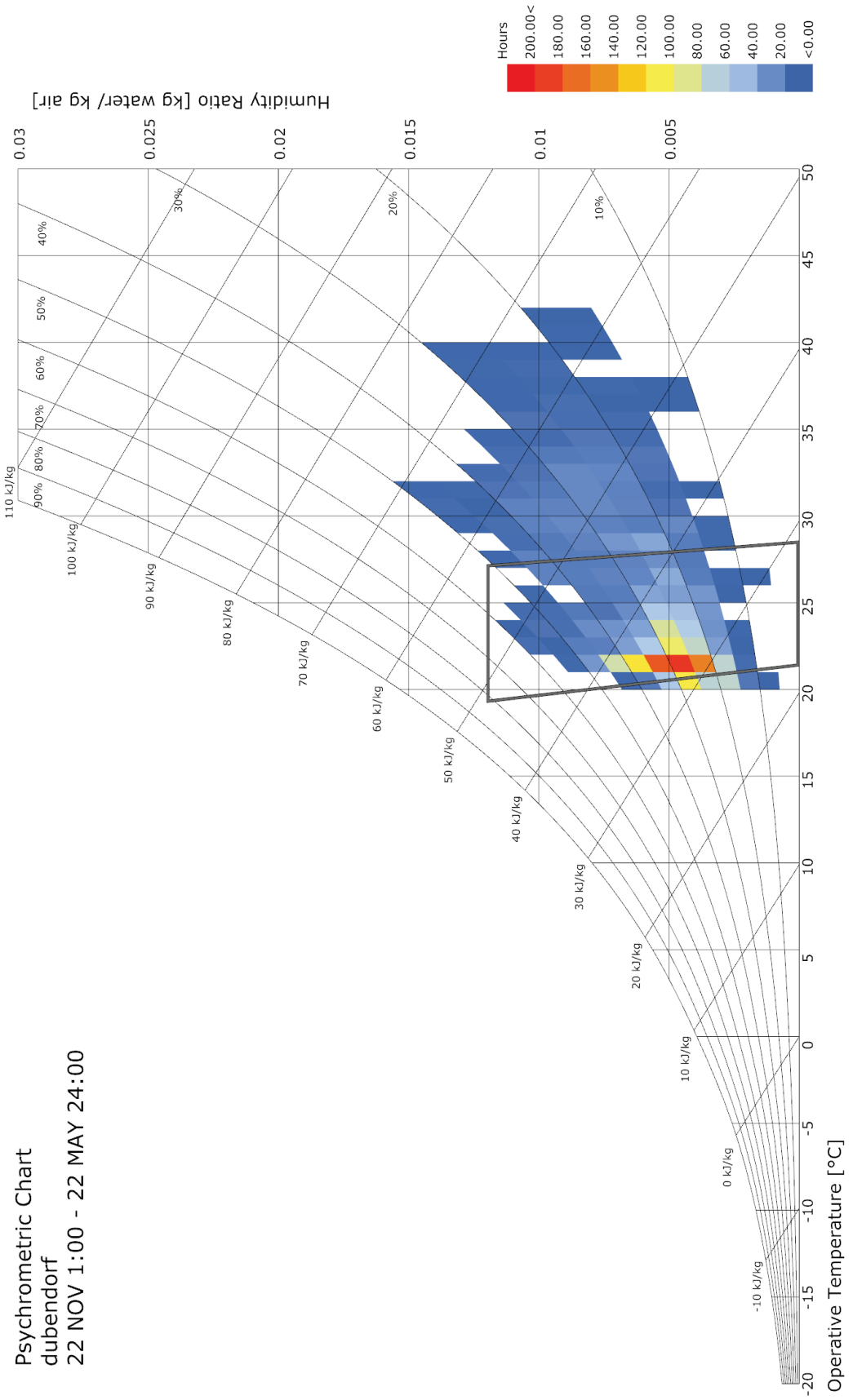

Comfortable time ratio	88 %

Figure 9-3: comfort diagram for the heating season in SolAce, simulated data.

10 Final Discussion

By looking at the overall energy needs for space heating across different calculation methods, a sound uniformity around the value of 28 kWh/m^2 year was observed.

Heated Floor Area	A_e	94	m^2	*from 22.11.2018 to 22.05.2019	547 days

GROSS VALUE	energy need	design phase	Dynamic (TRY)	monitoring*	
Space heating energy needs	Q_h	2684	2628	2516	kWh

ENERGY INTENSITY	energy need	design phase	Dynamic (TRY)	monitoring*	
Space heating energy intensity	E_h	29	28	27	kWh/m^2

Based on the solar thermal energy generation profiles (part III), one can compare the annual heating energy needs (at an hourly resolution) with the potential solar thermal supply, which would be obtained by connecting the solar thermal circuit to the space heating heat exchanger. The monthly bar plot shown in Figure 10-1 illustrates that almost twice the annual energy needed for space heating can be produced by the solar collectors, which currently cover barely the domestic hot water needs on an annual basis (see Part III).

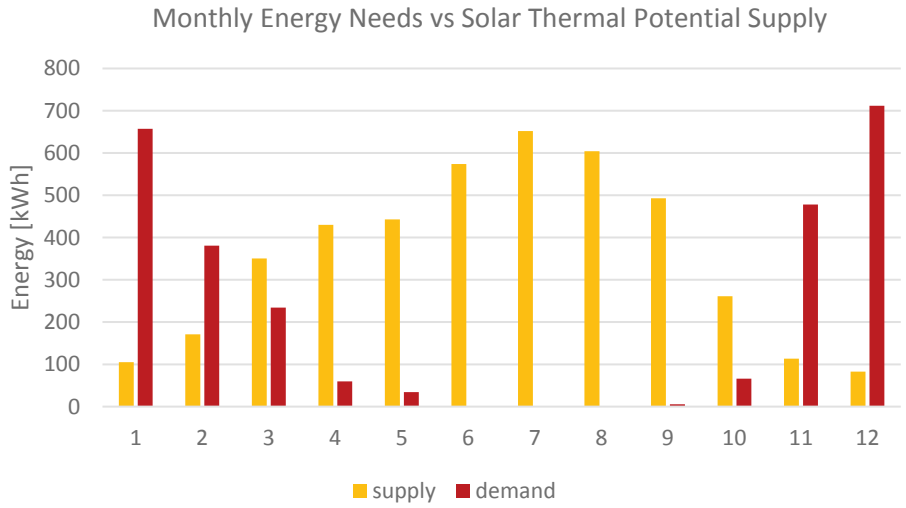

Simulated annual energy needs (EnergyPlus)	2628 [kWh]
Simulated annual solar thermal supply (Polysun)	4280 [kWh]

Figure 10-1: Monthly energy needs vs solar thermal potential supply, by connecting the solar thermal circuit to the space heating exchanger

Part III. Domestic Hot Water

11 Domestic Hot Water Needs

The SolAce unit has the particularity of being a multi-functional space: the unit can indeed be used as a workspace or as a living unit. It was therefore designed to provide the services required for both types of assignment.

This particularity implies a greater complexity in the modeling of the hot water needs of the unit. These are also significantly affected by user behavior and unit occupancy. Since its commissioning, the use of SolAce as living space has been sporadic, while being more used as workspace. This is reflected clearly in the monitoring of water consumption. Figure 11-1 shows the water consumption measured on the day of May 16, 2019, when a group of LESO-PB researchers went on site to perform various activities in the unit. This day reflects the presence of occupants in SolAce, as opposed to the day of 15 May 2019, for example, when the unit was unoccupied and when no water consumption was observed.

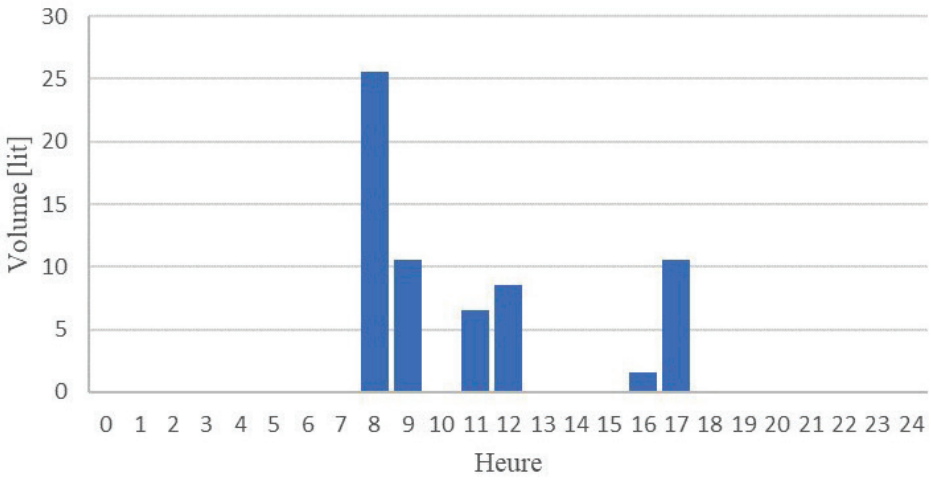

Figure 11-1: hourly domestic hot water consumption on 16th May 2019

It is important to underline that the measured water consumption includes both cold water consumption (CW) and domestic hot water consumption (DHW). The water meter therefore measures the overall water consumption of the unit. In order to evaluate more accurately the behavior of the unit in relation to the consumption of hot water, the addition of a flow meter dedicated solely to the DHW has been envisioned.

At present, two methods for calculating DHW requirements will be described. The first is to evaluate the needs according to the measured water consumption of the unit (calculation of the point of view "consumer") and the second is to determine these needs according to the energy delivered by the different heat sources (calculation of the point of view "producer").

11.1 Method 1 – Consumer

The first method is to assess the need for DHW needs according to a consumption profile specific to SolAce.

Table 5 below shows the consumption measured by the flow meter of the unit for each month since it was commissioned. The Christmas holidays were deducted from the number of days considered for the months of December and January, no water consumption was observed during this period.

	Number of days included in calculation	Measured values [l]	[l/day]
October 2018	9	128	**14.2**
November 2018	30	575	**19.2**
December 2018	21	296	**14.1**
January 2019	25	576	**23.0**
February 2019	28	454	**16.2**
March 2019	31	546	**17.6**
April 2019	30	509	**17.0**

Table 5. Measured domestic hot water consumption in the unit

We observe that water consumption is relatively stable over the months; this makes it possible to evaluate an average consumption of 17.3 [l / day]. This value corresponds to the daily water requirements of SolAce. However, according to statistics, residential water consumption in Switzerland is estimated at 160 [l / (pers day)] [8] and according to SIA 385/2, the consumption of DHW is 40 [l / (pers day)]. This makes it possible to define a ratio applicable to the consumption of SolAce.

$$V_{WW} = 17.3 \cdot \frac{40}{160} = 4.3\ [l/day]$$

As a reminder, the SIA 380/1 standard gives the method for calculating DHW requirements (Q_{ww}). These are expressed as follows:

$$Q_{WW} = \frac{\rho_w \cdot c_w \cdot V_{WW} \cdot (\theta_{WW} - \theta_{CW})}{A_E}\ [\frac{kWh}{m^2\ year}]$$

Assuming $\rho_w \cdot c_w$ [MJ/(m^3 K)] is the volumetric thermal capacity of water, V_{WW} is the volume of needed DHW, θ_{WW} is the hot water temperature at the extraction node, θ_{CW} is the cold water temperature as when it is supplied to the building, A_E is the heated floor area. By considering a hot water temperature equal to 55 °C and a cold water temperature of 15 °C, Q_{ww} reaches 0.7 [kWh/(m^2 year)] or 73 [kWh/year]. The obtained value is considerably lower than the annual reference values given by SIA 380/1, which amount to 14 [kWh / (m^2 year)] for housing and 7 [kWh / (m^2 year)] for administrative buildings. The reason is related again to the low occupancy rate of the unit.

11.2 Method 2 – Producer

DHW requirements can also be estimated from the energy transmitted to the hot water tank. The latter is powered by both the thermal collectors and the NEST energy Hub. The thermal losses of the hot water tank (Q_p) subtracted from the energy brought to the hot water tank (Q_{st}) correspond to the DHW requirements of the unit (Q_{ww}).

$$Q_{WW} = Q_{st} - Q_p$$

The thermal losses of the tank have been estimated at 377 [kWh / year], by knowing its size and insulation characteristics from the technical sheet. The energy added to the tank is the sum of the energy delivered by the NEST energy Hub ($Q_{Hub \rightarrow st}$) and the one delivered by the solar thermal collectors ($Q_{sol \rightarrow st}$).

$$Q_{st} = Q_{\mathrm{Hub} \rightarrow \mathrm{st}} + Q_{\mathrm{sol} \rightarrow \mathrm{st}}$$

The amount of energy delivered by the e-Hub to the tank is measured directly by the P890 flow meter (see datapoints diagrams). However, the amount of energy delivered by the solar thermal collectors

to the tank was not measured as such. It must be inferred from the total solar thermal output ($Q_{sol,\,tot}$) (heat meter P891) and the energy transmitted from the solar collectors to the e-Hub ($Q_{sol \rightarrow Hub}$).

$$Q_{\mathrm{sol}\,\rightarrow \mathrm{st}} = Q_{\mathrm{sol,tot}} - Q_{\mathrm{sol}\,\rightarrow \mathrm{hub}} \;\Rightarrow$$

$$Q_{\mathrm{st}} = Q_{\mathrm{Hub}\,\rightarrow \mathrm{st}} + Q_{\mathrm{sol,tot}} - Q_{\mathrm{sol}\,\rightarrow \mathrm{hub}}$$

Measured values for all the previous listed data points are listed in

Table 6.

Data point	Measured value [kWh]
$\boldsymbol{Q_{\mathrm{sol,tot}}}$	774
$\boldsymbol{Q_{\mathrm{sol}\,\rightarrow \mathrm{hub}}}$	630
$\boldsymbol{Q_{\mathrm{Hub}\,\rightarrow \mathrm{st}}}$	626
$\boldsymbol{Q_{\mathrm{st},monitored\ period}}$	**770**

Table 6. Measured values allowing for calculation of the energy transmitted to the hot water tank

The obtained value can be extrapolated to the entire year given the number of operating days considered in the above-mentioned calculation and assuming a constant DHW consumption throughout the year. The currently covered period ranges from September 24, 2018 to April 5, 2019, which corresponds to 194 days of operation. The energy transmitted to the tank is therefore 1449 [kWh / year]. DHW requirements can now be calculated as follows.

$$Q_{WW} = Q_{st,TRY} - Q_p = 1449 - 377 = 1072\ [\frac{kWh}{year}]$$

As such, domestic hot water energy intensity is equal to 11.4 [kWh/(m^2 year)]. This outcome is considerably higher than the one calculated according to the first method. A first reason is identified in a defect of the sensor detecting the energy transmitted from the Hub to the tank (QHub → st). Most probably, this data point was incorrectly configured during the commissioning of the unit, the monthly measurement being returned instead of the hourly measurement. A second reason that may explain this wide variation is the fraction of DHW consumption compared to the total water consumption in SolAce, (i.e. the ratio 40/160, see above): however, a higher share of total measured water consumption could actually correspond to the DHW consumption. Finally, various hypotheses underlying the calculation of the tank's thermal losses can influence the results.

This demonstrates the importance of adding a water flow meter intended solely for DHW consumption, as mentioned above. Nevertheless, the DHW requirements calculated according to the first method are preferred as for the rest of the report. In fact, an established measure of water flow is ideal for solar thermal production simulations.

12 Solar Thermal Production

12.1 Solar thermal system characteristics

The SolAce unit is equipped with solar thermal collectors intended to cover DHW needs. The solar collectors are positioned on the south-east facade of the building, oriented at 119° relative to the geographical North. The whole system covers a gross area of 19.5 m^2 and a net area of 18 m^2.

Figure 12-1 shows the schematic diagram relative to the system, which includes the following elements:

- 1: Solar thermal collectors

- 2: DHW tank
- 3: External heat exchanger
- P1: Solar circulation pump
- P2: Hub circulation pump
- V1: 3-way valve for solar production
- V2: 3-way valve for charging the DHW tank
- V3: 6-way switching valve
- S1: Temperature sensor - Solar collector
- S2: Temperature sensor - DHW tank top
- S3: Temperature signal - DHW tank bottom

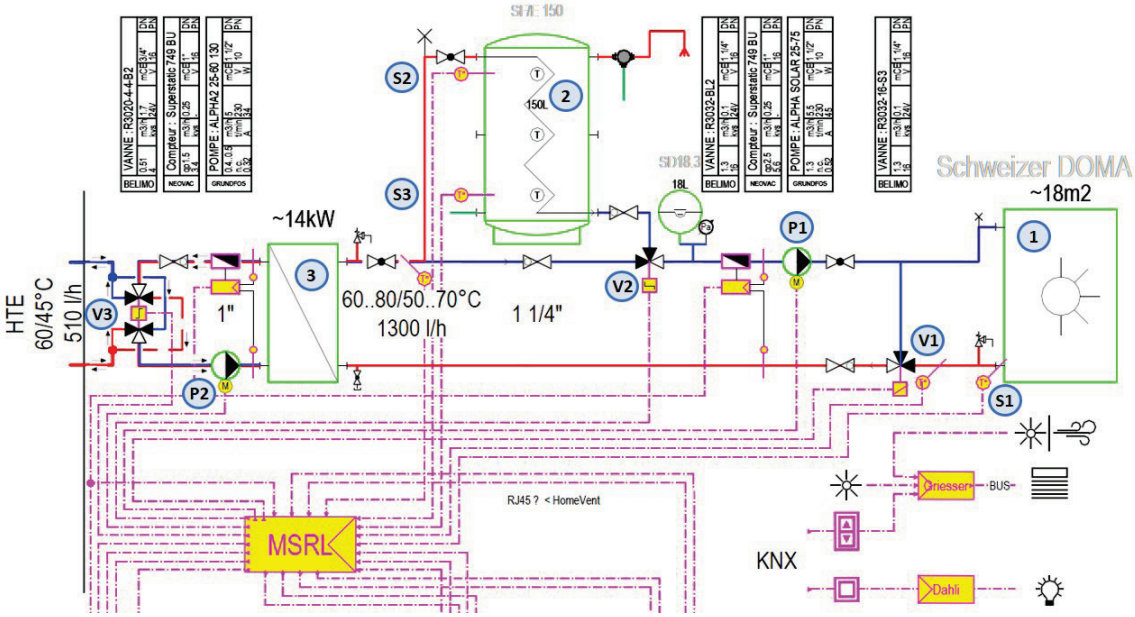

Figure 12-1: solar thermal system schema.

As shown in this technical diagram, the solar system of the SolAce unit has a relatively simple design. In fact, it consists of only three main elements (the collectors' field, the hot water tank and the external heat exchanger) and has no direct interaction with the heating system. The latter point is essential: the solar collectors provide power to the high temperature water loop of the Hub and the DHW tank, but not to the heating system of the unit. However, since the e-Hub is also the source of heating energy, there is an indirect link between solar thermal generation and heating consumption (although both uses rely on two different temperature loops).

Although the installation includes few technical elements, the overarching control algorithm is complex. For example, when the hot water tank meets the set point temperature and the collectors produce excess heat, the latter is re-injected into the building's e-hub via a 6-way valve allowing for the inversion of the flow's direction. This practice is not often used on conventional systems: few are the cases in which a "heat sink" can receive excess heat, such as district heating for example.

In addition, the internal exchanger of the DHW tank lies along the entire tank's height dimension. It allows transferring heat from both the solar collectors and the e-Hub. This is an uncommon practice since the auxiliary heat generator can inhibit the operation of solar collectors, the former being often more responsive than the latter. The solar collectors are usually connected to a heat exchanger located on the lower portion of the tank, while the auxiliary heat generator acts on the upper storage volume.

12.2 Solar thermal system simulation

The simulation of the solar thermal production is carried out thanks to the POLYSUN software [9]. Figure 12-2 shows the modeling of the solar thermal system of the unit using the software.

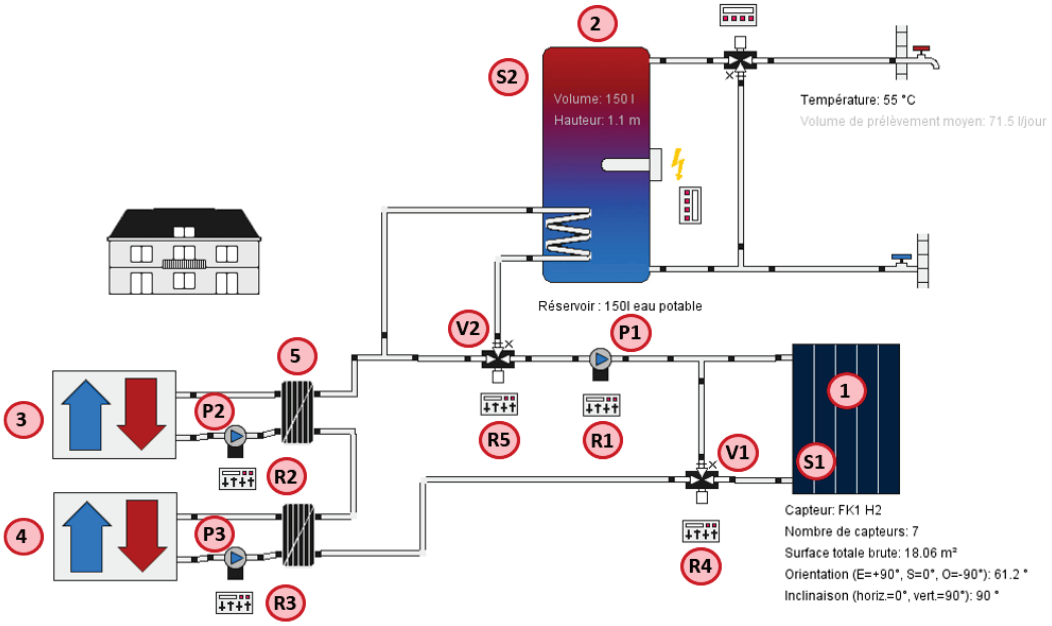

Figure 12-2: schema of the system simulated in Polysun ®

The elements indicated with red pellets in the figure above are as follows:

- 1: Solar thermal collectors
- 2: DHW tank
- 3: Hub - source
- 4: Hub - absorber
- 5: External heat exchanger
- P1: Solar circulation pump
- P2: Hub circulation pump - source
- P3: Hub-absorber circulation pump
- V1: 3-way valve for solar production
- V2: 3-way valve that powers DHW tank
- S1: Temperature sensor - Solar collectors
- S2: Temperature sensor - DHW tank top
- R1: Solar pump regulator
- R2: Hub-side pump regulator - source
- R3: Hub-side pump regulator - absorber
- R4: Three-way valve regulator for solar generation
- R5: Regulator of the three-way valve to power the DHW tank

The DHW needs calculated in section 11 are used as input to the simulation model. However, some adaptations had to be made to the model to take into account the complexity of the energy Hub. As such, the characteristics of each modeled element, as well as the regulation aspects, are detailed below.

12.2.1 Solar thermal collectors

	Model	**Reality**

Type	Schweizer - FK1 H2	Schweizer - Doma Flex
Surface [m2]	18	18
Orientation (Nord = 0°) [°]	118	118
Tilt [°]	90	90

The Doma Flex solar collectors installed on the facade are not part of the POLYSUN products catalog. Thus, a product with the same characteristics and the same manufacturer was chosen.

12.2.2 Hot water tank

	Model	**Reality**
Type	Standard	hpa - SF/E 150 lit
Volume [l]	150	150
Heat exchanger active height [cm]	30	40

A standard model from the POLYSUN base catalog is used for the DHW tank. Note that the electric heater (auxiliary heat generator) is manually disabled, in order to consider exclusively the Hub as an auxiliary heat generator.

The active height of the internal heat exchanger is important to define the hot water stratification in the storage tank. Usually, the exchanger occupies the lower third of the storage tank: the two thirds above will be raised to the same temperature by convection, which allows having a sufficient amount of water meeting the set point. This is not the case if the exchanger is active over the entire height of the storage tank. In this situation, only a small volume located at the top of the tank reaches the desired temperature.

The height of the heat exchanger installed inside tank is calculated from the data sheet. The height of the "coil outlet" with respect to the ground is 640 [mm] and that of the "return coil" is 240 [mm], which makes the exchanger active height equal to 40 [cm].

12.2.3 Energy Hub – source

	Model	**Reality**
Inlet temperature [°C]	45	45
Outlet temperature [°C]	60	60
Flow [l/h]	510	510
Power [kW]	8.9	8.9

The "absorber / energy source" component makes it possible to model a heat source or a heat sink, that is to say an entity for delivering or absorbing heat. A common example of a heat source is the district heating network (DH). As mentioned in the description of the installation, the NEST high temperature loop (HTE) acts as both a heat source and a heat sink, the direction of the flow being regulated by the 6-way valve. The modeling of this valve is not possible with POLYSUN, thus two components "absorber / source of energy" are used respectively.

The solar thermal system is connected to the HTE network of the NEST, operating at a temperature range of 45/60 [° C]. In addition, the "absorber / energy source" component requires a nominal power. The latter is calculated as follows:

$$P = c \cdot q \cdot \Delta T = 4180 \cdot \frac{510}{3600} \cdot (60 - 45) = 8883\ [W] = 8.9\ [kW]$$

Where c [J/(lit K)] is the volumetric thermal capacity of water, q [lit / s] is the nominal water flow through the pump retrieved from the technical sheet, ΔT [°C] is the temperature gradient between inlet and outlet water.

12.2.4 Energy Hub – absorber

	Model	**Reality**
Inlet temperature [°C]	60	60
Outlet temperature [°C]	45	45
Flow [l/h]	510	510
Power [kW]	-8.9	-8.9

The characteristics of the component absorbing the excess solar heat are the same as those of the previous component, with the exception of the input / output temperatures which are inverted and imply a negative sign power.

12.2.5 External heat exchanger

	Model	**Reality**
Type	Standard	Kaori - BPHE H29-24
Heat transfer capacity [kW]	14	14
Specific heat transfer capacity [W/K]	700	700

A supplementary heat exchanger is used in the unit either to supply heat from the e-Hub to the storage tank or to inject excess heat to the latter. The use of a heat exchanger is also necessary to dissociate the NEST building hot water loop from the local one of SolAce, which do not carry the same type of fluid. The heat of the solar thermal plant is conveyed thanks to a propylene-glycol based heat transfer fluid. This prevents the pipes from freezing in the solar collectors when the outside temperature drops below zero degrees Celsius.

To model the heat exchanger correctly, its specific heat transfer capacity in [W / K] must be determined. As such, the heat transfer capacity of 14 [kW] characterizing the exchanger in the data sheet is divided by the temperature difference on the SolAce side. According to the HVAC technical scheme this temperature difference is 20 [K]. The specific heat transfer capacity is therefore 700 [W / K].

12.2.6 Pumps

Pump	**Water flow [lit /h]**
Solar loop pump	1300
Hub loop pump	510

The main characteristic of modeled pumps is the flow they convey, mentioned in the above table. The second important element is their operation control, which goes beyond a simple timer and allows for a variable flow.

12.2.7 Flow control

Control is a key element in the operation of the solar thermal system, regulating all the dynamic behavior of the plant (switching on / off the circulators, positioning the valves, etc.). It is also an aspect that can be optimized without additional material costs once the installation realized.

At present, the regulation of the HVAC system, inclusive of heating, cooling, ventilation and DHW was programmed by the company "AMSTEIN + WALTHERT". The regulation of the various components of the plant is mainly based on the temperature output from the S1 and S2 sensors (see Figure 12-2), but other state values are also used. The table below describes how the control aspects are modeled. The anti-legionella function has not been included, as the impact on the solar production of the facility is low. Note also that Boolean operators are used to relate the different equations, this representing the actual operation of the control systems.

Status	Control R1	Control R2	Control R3	Control R4	Control R5
ON	S2 < 45 OR S1 >= S2 + ΔT	S2 < 45 AND S1 < S2 + ΔT	S1 >= 70 AND S2 >= 65	S1 >= S2 + ΔT	S2 >= 65
OFF	S2 >= 56 AND S1 < S2 + ΔT	S2 >= 56 OR S1 >= S2 + ΔT	S1 < 70 OR S2 < 65	S1 < S2 + 3	S2 < 45 OR S1 >= S2 + ΔT

For all modeled controls, the variable ΔT is equivalent to 5 [° C]. It represents the switching differential, also known as the switching hysteresis, which corresponds to the temperature difference between the collector field and the tank that triggers the solar pump. Control R1 has the priority over control R2 to avoid conflicts between the hub and the solar collectors' production. Control R4 closes the valve when the temperature of the collectors drops below that of the storage tank plus 3 [° C] to account for the distribution losses (the progressive closing is not accounted for in the model).

13 Results

After being calibrated on typical winter and summer days using the appropriate monitored variables, the simulation model has been run throughout an entire Test Reference Year (TRY). The total energy delivered to both the storage tank and the energy hub during the TRY is equal to 2441 [kWh/year]. Monthly results can be observed in the table below:

Month	Qsol→Hub [kWh]	Qsol→st [kWh]	Qsol,tot [kWh]	Qhub→st [kWh]	f_{sol} [%]
Jan	17.5	38.6	56.1	37.7	50.6
Feb	53.3	50.7	104	21	70.7
Mar	133	80	213	10.9	88.0
Apr	162	93	255	0	100.0
May	140	89	229	9.3	90.5
Jun	183	102	285	0	100.0
Jul	244	110	354	0	100.0
Aug	254	96	350	9.8	90.7
Sep	232	86	318	8.2	91.3
Oct	103	60	163	19.4	75.6
Nov	33.8	37	70.8	34.9	51.5
Dec	16.1	26.2	42.3	50.8	34.0
Annual	**1572**	**869**	**2441**	**202**	**81.1**

The solar fraction, representing the ratio between the energy needs and the energy production, corresponds to the energy supplied to the storage tank by the solar collectors in relation with the total energy delivered to the tank. As such, the solar fraction f_{sol} is calculated as follows:

$$f_{sol} = \frac{Q_{sol \to st}}{Q_{sol \to st} + Q_{Hub \to st}}$$

As shown in Figure 13-1, the solar production delivered to the DHW tank is higher during the summer months than during the winter months, reaching a coverage rate of 100% for the months of April, June and July (as expected).

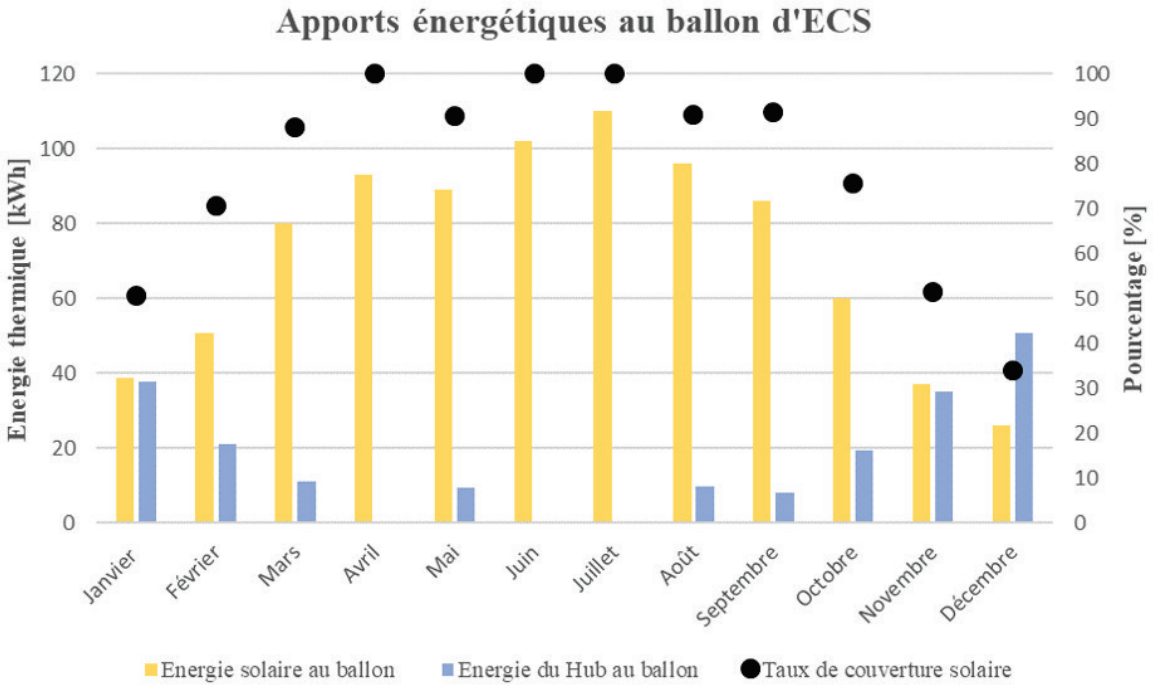

Figure 13-1: monthly results of the solar thermal simulation

The monitored production for the period ranging from 24 September 2018 to 5 April 2019 (194 days) is 774 [kWh]. This outcome can be extrapolated to the entire year by knowing the incident solar radiation on collectors' plane during the monitored period and during the entire year respectively. Such values can be retrieved from the meteorological data of the Test Reference Year (TRY), corrected to take the appropriate orientation and eventual shadings into account. The sky matrixes built in Radiance for the space heating simulation conducted previously in Energy Plus (Part II) serve for this purpose, and the extrapolation is made as follows:

$$Q_{sol,tot} = Q_{sol,monitored\ period} \cdot \frac{E_{monitored\ period}}{E_{annual}} = 774 \cdot \frac{4663}{13053} = 2181\ [\frac{kWh}{year}]$$

The monitored solar energy production at SolAce is then comparable to the results issued from the POLYSUN simulation. The simulation overestimates the energy produced by about 10%.

Heated Floor Area	A_e	94	m^2	*from 22.09.2018 to 05.04.2019	547 days

GROSS VALUE	energy need	design phase	Dynamic (TRY)	monitoring*	Annual extrapolation	
Domestic Hot Water energy needs	Q_{hw}	2034	-	770	1072	kWh
Solar thermal production (HTE)	$Q_{sol,tot}$	4569	2441	774	2181	kWh

ENERGY INTENSITY	energy need	design phase	Dynamic (TRY)	monitoring*	Annual extrapolation	
Domestic Hot Water energy needs intensity	E_{hw}	22	22	8	11	kWh/m^2
Solar thermal production energy intensity (HTE)	$E_{sol,tot}$	49	26	8	23	kWh/m^2

14 Discussion

Some modifications may improve the operation of the solar thermal plant and increase the solar production:

1. A nighttime delay can be programmed for the pump on the NEST heat network. This would avoid any possible conflict between the heat input from the e-Hub and from the solar collectors during the day.
2. Hysteresis triggering on and off the system can be optimized. Currently, the first is set at 5 [° C] and the second is set at 3 [° C]. The latter could be lowered to 2 [° C] given the short length of the distribution pipes.
3. Flow rates of pumps could be optimized. It was noticed during a SolAce visit that the P1 solar circulation pump was oscillating between on and off, especially during the morning. This could be avoided if circulators conveyed the appropriate heat flow.

Beyond these modifications to the controls of the plant, optimizing the operational temperature range of the solar collectors can considerably increase the energy production. Currently, the energy produced by the collectors is mainly used to supply the DHW tank. As such, only a water flow temperature of a minimum of 70 [° C] guarantees the injection of the solar excess into the Hub. The heat exchange between a water flow in a temperature range between 45 and 65 [° C] and the NEST MTE network (instead of the HTE network) could improve the efficiency of the system. In addition, this modification would not require significant efforts in terms of space and would not generate excessive financial costs. Such implementation would imply a slight modification of the hydraulic system. It is therefore a very interesting alternative (see section 10).

Part IV. Electricity

15 Electricity needs

The electricity needs are determined using the absorbed power of the electrical appliances and lighting installed in SolAce and their usage profile. The table below shows the installed luminaires and their characteristics (based on the documentation of the company "Regent").

Luminaire	Zone	Nb	Unit power [W]	Total power [W]
Solo slim led	Mixed use space	12	30	**360**
Solo slim led	Mixed use space	2	60	**120**
Echo 210 led	Mixed use space	5	30	**150**
Minilobby	Bedroom	1	15	**15**
Zena led	Bedroom	8	15	**120**

The installed lighting power is 765 [W], which represents a lighting power density of 9 [W / m2] for the whole unit. The table below shows the consumption of computers and appliances installed in SolAce. These consumptions were calculated according to the standard SIA 380/4.

Electric appliance	Number	Annual electricity consumption [kWh/an]
PCs with LED screen	4	94
Fridge and freezer	1	238
Washing machine	1	112
Oven	1	30
Kitchen	1	260

Given the hypotheses explained in sections 7.3.2 and 7.3.3, the total yearly electricity consumption can be determined, and amounts to 2056 [kWh/year].

The actual electricity consumption is measured using different electricity meters in the unit. The meters in question are named U25E1 / P890, U25E1 / P891, U25E1 / P892, U25E1 / P893 and are illustrated in the electrical monitoring diagram. The measured value for the monitoring period (24 September 2018 to 5 April 2019) amounts to Qel, monitored period is equal to 844 [kWh]. This value can be extrapolated linearly to the year, knowing the number of days of the considered period.

$$Q_{el,tot} = 844 \cdot \frac{194}{365} = 1588\ [\frac{kWh}{year}]$$

16 Photovoltaic system

Renewable electricity generation is provided by a set of photovoltaic modules installed on the south-west facade of SolAce. The photovoltaic cells are laminated Kromatix® glass to ensure a better architectural integration. Indeed, the use of such glass makes it possible to homogenize the facades of the unit, including the southeast facade, where the solar thermal collectors are located. The technical data related to the photovoltaic modules are presented in the table below. These values were used to simulate the annual photovoltaic production.

Feature	Symbol	Unit	Value
Number of modules	n_{mod}	[-]	11
Module - height	h_{mod}	[m]	1.39
Module - width	l_{mod}	[m]	1.12
Gross modules surface	S_b	[m2]	17.1
Net modules surface	S_n	[m2]	12.3
Nominal peak power per module	P_u	[Wp]	194
Orientation	-	[°]	-151
Tilt	-	[°]	90
Incident solar radiation	-	[kWh/(m2· an)]	845

The above data come partially from the PVsyst report provided by Dr Nicolas Jolissaint from SwissINSO, the company producing the Kromatix glass. From these data, it is possible to determine the conversion efficiency of the photovoltaic modules. The latter is evaluated at standard operating conditions, i.e. an incident irradiation of 1000 [W / m2] and a temperature of 25 [° C].

$$\eta = \frac{P_u \cdot n_{mod}}{S_n \cdot 1000} = \frac{194 \cdot 11}{12.3 \cdot 1000} = 17.3\ \%$$

The total power of the photovoltaic system is calculated from the number of modules and their unit peak power. This value will be used in particular to determine the embodied energy of the solar plant (Part V).

$$P_{PV,tot} = n_{mod} \cdot P_u = 11 \cdot 194 = 2.13\ [kWp]$$

The total yearly production simulated in PVSyst amounts to 1574 [kWh/year]. The corresponding monitored value is retrieved from an electricity meter. The meter in question is labeled U25E3 / T100 (see electrical monitoring diagram). The monitoring period ranges from 24 September 2018 to 5 April 2019. During this period, the photovoltaic production amounts to Q_{PV}, monitored period equals to 697 [kWh]. This outcome can be extrapolated to the entire year by knowing the incident solar radiation on modules' plane during the monitored period and during the entire year respectively. Such values can be retrieved from the meteorological data of the Test Reference Year (TRY), corrected to take the appropriate orientation and the eventual shading into account. The sky matrixes built in Radiance for the space heating simulation conducted previously in Energy Plus (Part II) serve this purpose, and the extrapolation is made as follows:

$$Q_{PV,tot} = Q_{PV,monitored\ period} \cdot \frac{E_{monitored\ period}}{E_{annual}} = 697 \cdot \frac{6323}{13221} = 1457\ [\frac{kWh}{year}]$$

The obtained simulated value complies with the measured value. However, the latter is 7% lower than the simulated. This may be due to the difference between meteorological data available for simulation (TRY) and reality.

Heated Floor Area	A_e	94	m^2	*from 22.09.2018 to 05.04.2019	547 days

GROSS VALUE	energy need	design phase	Dynamic (TRY)	monitoring*	Annual extrapolation	
Electricity needs	Q_{el}	2068	2056	844	1588	kWh
PV production	$Q_{PV,tot}$	1587	1574	697	1457	kWh

ENERGY INTENSITY	energy need	design phase	Dynamic (TRY)	monitoring*	Annual extrapolation	
Electricity needs intensity	E_{el}	22	22	9	17	kWh/m^2
PV production energy intensity	$E_{PV,tot}$	17	17	7	16	kWh/m^2

Part V. Embodied energy

17 Thermal envelope

In order to assess the embodied energy entailed by the life cycle of the thermal envelope, it is necessary to determine the quantity of each material that composes it. This quantity depends on the reference unit associated with the materials in the KBOB database, a Swiss federal inventory of constructional materials' life cycle impacts. The reference unit is the one in which the environmental impacts are evaluated in the KBOB database [10]. As an example, the latter reports the embodied energy of a double-glazed window per area [m^2], whereas the embodied energy of a solid wood element is related to the mass [kg]. The mass of a building component in [kg] is inferred from the technical data sheet relative to the density of its composing material and from its volume.

Surface extensions are extracted from the 3D model and summarized in the table below. The floor and ceiling surfaces differ by 0.9 [m^2], due to the offset of the daylighting section on the south-west facade.

Construction element	Surface [m^2]
Outdoor exposed walls (opaque)	46.6
Outdoor exposed windows	41.2
Interior walls (opaque)	88.3
Entrance door	3
Floor	95.2
Ceiling	96.1

By knowing the thickness and the surface of each layer of the thermal envelope, the volume of each material can be calculated. As mentioned previously, the mass of the elements is deduced by using the density of the respective materials. The mass of the entrance door is set arbitrarily at 100 [kg] and the mass of the windows is calculated using a mass coefficient of 40 [kg / m^2]. Results are shown in the table below.

Construction material	Volume [m^3]	Mass [kg]
Concrete slab	4.8	8806
Agglomerated wood panel (OSB)	7.2	5010
PE vapor barrier	0.16	116
Wood fiber insulation	77.8	10884
Spruce tiles	10.9	5243
3-ply panel	2.6	1557
FERMACELL panel	4.7	4205
Wood panel Kronotec WP50	0.7	479
Eurocol LiquidDesign Resin	0.6	238
Windows	1.9	1648
Entrance door	0.12	100
TOTAL	**111.3**	**38236**

The total mass of the building components of SolAce is equal to approx. 40 tons, without considering the HVAC infrastructures, the sanitary installations, the piping, etc. The pie charts below show the volume and mass breakdown of the SolAce components.

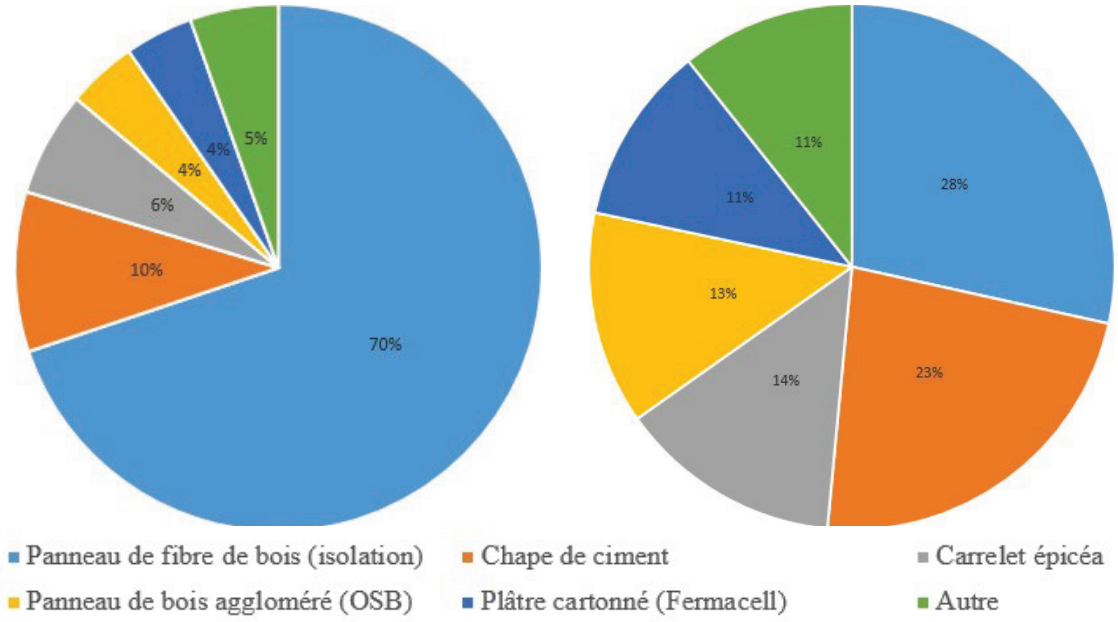

Construction material	KBOB material	Lifespan (years)
Concrete slab	Concrete slab 85 mm	60
Agglomerated wood panel (OSB)	Agglomerated wood panel (OSB), PF glue, humid zone	60
PE vapor barrier	PE vapor barrier	60
Wood fiber insulation	Pavatex soft fibers board	60
Spruce tiles	Spruce / fir / larch solid wood, air dried, planed	60
3-ply panel	3-layer solid wood panel, PVAc glue	60
FERMACELL panel	Gypsum plasterboard	60
Wood panel Kronotec WP50	Medium Density Fibreboard (MDF), UF glue	60
Eurocol LiquidDesign Resin	Casting coating with 2 comp. residential / admin. (PU epoxy resin), 2 mm	30
Windows	Triple glazing, ESG / ESG glass, U <0.6 W / m^2K	30
Entrance door	Internal wooden doors	30

Each material identified in the thermal envelope is linked to a material from the KBOB database. This is shown in the above table. The KBOB database indicates the embodied energy of each material, including construction and dismissing impacts. However, in order to compare the amount of embodied energy with the operational energy, the former must be related to an annual value. The technical specification SIA 2032 serves for this purpose: it defines the lifespans to account for each building element, depending on its own functional group, within the "Construction Cost Code". For example, the excavation work (group B) has a lifespan of 60 years, while the interior set-ups (group G) have a lifespan 30 years. These are hypothetical values and the lifespan of the building elements can vary considerably in practice. This phenomenon is particularly significant in a semi-temporary constructions such as SolAce. The lifespans of the thermal envelope is also presented in the above table.

Now that the materials have been identified, their quantity determined and their lifespan specified, it is possible to calculate the embodied energy of the thermal envelope. For this, the following equation is used:

$$EE_i = \frac{EE_{i,KBOB} \cdot q_i}{a_i}$$

With EE [kWh/year] is the embodied energy of the element i, EE_{KBOB} [kWh/ref. unit] embodied energy of the associated KBOB material, q [ref. unit] the material quantity expressed in reference units, a [years] lifespan of the material. The different variables are listed in the table below. The total embodied energy of the envelope amounts to 1789 [kWh/year] and breaks down to the different shares illustrated in the pie chart.

As shown in the latter, one-third of the embodied energy in the SolAce envelope is due to the wood fiber insulation. This may be surprising, wood being usually used in low environmental impact constructions. The explanation lies in the fact that the wooden insulation represents 70% of the volume and 28% of the mass of the thermal envelope.

The windows also represent nearly a third of the embodied energy of the envelope, due to the amount of surface they occupy on outer walls (nearly half). The lifespan of windows being half of the opaque walls also plays a role in this concern.

The last third of the embodied energy is due to the rest of the materials. As for the share of embodied energy associated with the materials "chipboard – agglomerated wood panel OSB" and "FERMACELL", an observation can be made. In fact, despite the total mass of these two materials is comparable, the embodied energy resulting from OSB panels is more than double the one of plasterboard panels (FERMACELL panel), while the former are mainly made of wood. The embodied energy values from the KBOB data are equal to 1.4 [kWh / kg] for FERMACELL panels and 2.8 [kWh / kg] for OSB panels. The reason for this remarkable difference lies in the composition of FERMACELL panels, which are made of plaster and recycled cellulose fibers. These two natural components are mixed and bound by addition of water, then compressed to obtain a rigid plate. This process is characterized by a rather low ecological footprint.

Construction material	**RU**	**$EE_{i,KBOB}$**	**a_i**	**q_i**	**EE_i**
Concrete slab	[kg]	0.3	60	8806	41.2
Agglomerated wood panel (OSB)	[kg]	2.8	60	5010	230.4
PE vapor barrier	[kg]	24.8	60	116	48
Wood fiber insulation	[kg]	3.1	60	10884	569.6
Spruce tiles	[kg]	0.7	60	5243	60.3
3-ply panel	[kg]	3	60	1557	77.6
FERMACELL panel	[kg]	1.4	60	4205	94.6
Wood panel Kronotec WP50	[kg]	4.9	60	479	38.9
Eurocol LiquidDesign Resin	[m^2]	31.2	30	95.2	99
Windows	[m^2]	371	30	41.2	509.5
Entrance door	[m^2]	193	30	3	19.3

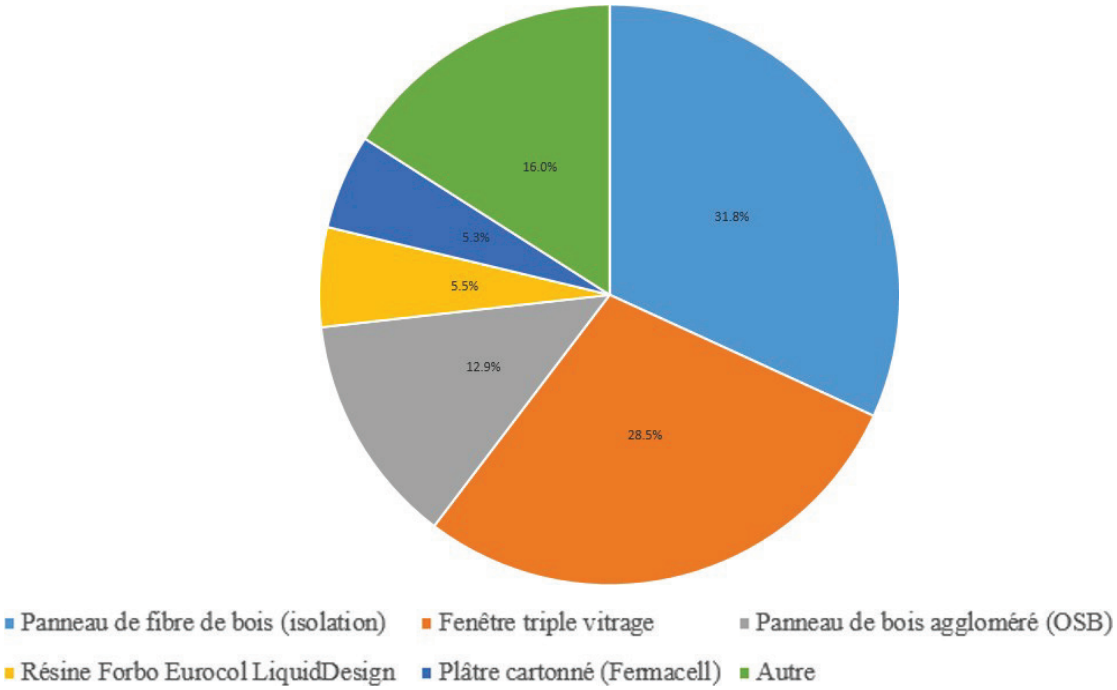

18 Solar collectors and PV modules

The KBOB database is used to determine the embodied energy of the solar thermal collectors and photovoltaic modules. As for photovoltaic panels, the database differentiates between installations on flat roofs, pitched roofs or facades: the reference unit is the kilowatt-peak [kWp]. Thus, the embodied energy associated with façade-integrated photovoltaics is multiplied by the peak power of the PV system, equal to 2.13 [kWp].

The lifespan of both solar thermal and PV panels ($a_{PV,\ ST}$) is set to 25 years. This reflects the current state of the art, although some components of the system may have a shorter lifecycle. This is the case of e.g. inverters, which typically last from 5 to 10 years. However, some PV systems are reported to last up to 40 years [11].

The embodied energy of the photovoltaic system (EE_{PV}) can therefore be calculated given the above data in the following way:

$$EE_{PV} = \frac{EE_{PV,KBOB} \cdot P_{PV,tot}}{a_{PV,ST}} = \frac{7460 \cdot 2.13}{25} = 636\ [\frac{kWh}{year}]$$

Concerning solar thermal collectors, the database determines the embodied energy values as a function of the gross area of the collectors' field in [m^2]. The database also distinguishes several types of systems, such as: flat plate collectors for domestic hot water supply of a single family house, flat plate collectors for space heating and hot water supply of a single family house, flat plate collectors for domestic hot water supply of an apartment, evacuated tubes collectors for space heating and domestic hot water supply of a single family house.

For the SolAce unit, the selected value corresponds to the domestic hot water supply in a single-family dwelling. In fact, the space heating and DHW systems are separated. As mentioned before, the gross area of the solar thermal collector field is 19.5 [m^2]. From this information, it is possible to calculate the embodied energy of the solar thermal collector field (EE_{ST}).

$$EE_{ST} = \frac{EE_{ST,KBOB} \cdot S_{ST,tot}}{a_{PV,ST}} = \frac{1140 \cdot 19.5}{25} = 889\ [\frac{kWh}{year}]$$

The embodied energy of solar thermal collectors is therefore nearly 40% higher than the one of photovoltaic modules. The main cause of this difference lies in the distribution pipeline and the heat storage included in the solar thermal system. Apart from the inverters, the photovoltaic modules do not have components affecting the amount of embodied energy other than the modules themselves. In addition, the difference in surface area of thermal panels (19.5 [m^2]) and photovoltaic panels (17.1 [m^2]) has an impact too.

Another impact comes from the use of rare materials, especially in the case of solar collectors. The latter employ copper whereas photovoltaic modules feature semiconductors such as silicon, gallium or arsenic. These rare materials must be extracted from remote mines, and then transported to the assembling line. This process has a considerable impact on embodied energy. For the purpose of this report, the impact of using Kromatix glass was not included in the calculation of embodied energy. As such, embodied energy may be underestimated as for solar conversion devices.

19 HVAC and sanitary components

The technical components considered for calculating the unit's embodied energy are the heating and ventilation systems as well as the sanitary elements; the heating system includes the radiating beams. With regard to the ventilation system, the KBOB database calculates the relative embodied energy according to the airflow to be renewed. In case of offices, data is available for flow rates of 1, 2, 4, 6 and 8 [m^3 / (h · m^2)]. The flow rate closest to 1.91 [m^3 / (h · m^2)], calculated in section 7.3.6, is 2 [m^3 / (h · m^2)]. The reference unit assumed for HVAC components is the heated floor area. The table below summarizes the chosen records in the KBOB database associated with the HVAC components.

	$EE_{tech,KBOB}$ [kWh oil eq / m^2_{HFA}]
Heat diffusion through the radiating beams	26.4
Office ventilation, sheet metal ducts, with airflow requirements = 2 [m^3 / (h · m^2)]	73.6
Sanitary installation - Office, low complexity, appliances and pipes included	19.6

As for the materials composing the thermal envelope, lifespans considered for the HVAC components (a_{tech}) are issued from the technical standard SIA 2032. The majority of the elements belonging to group D "technical installations" have a lifespan of 30 years. This is the case for heating and ventilation systems and sanitary installations. Thus, the embodied energy associated with the technical installations (EE_{tech}) can be calculated as follows.

$$EE_{tech} = \frac{EE_{tech,KBOB} \cdot HFA}{a_{tech}} = \frac{119.6 \cdot 94}{30} = 889\ [\frac{kWh}{year}]$$

20 Overall results

Given the above-mentioned assumptions, the embodied energy of the overall SolAce unit can be calculated. The latter corresponds to the sum of all contributions resulting from each element composing the unit. The table below summarizes the overall computation.

	Symbol	**Embodied energy [kWh/an]**	**Share [%]**
Thermal envelope	EE_{env}	1789	48.2
PV modules	EE_{PV}	636	17.3
Solar thermal collectors	EE_{ST}	889	24.2

Technical components	EE_{tech}	375	10.2
SolAce	**EE_{SolAce}**	**3688**	**100**

$$EE_{SolAce,spec} = 39.2\ [\frac{kWh}{m^2\ year}]$$

The embodied energy of SolAce is finally related to the heated floor area, returning an overall specific embodied energy of 39.2 [kWh/(m^2 · year)]. The following section discusses the compliance of the overall embodied energy with the label "Minergie-Eco".

21 Minergie-Eco

The Minergie-ECO label [12] is the benchmark for healthy and green buildings in Switzerland. The certification covers 80 criteria, 12 of which are considered as exclusive criteria, i.e. they must be fulfilled to obtain the certificate. Most of these criteria are assessed on a green-yellow-red color-code, according to a specific logic (derived from the Hermione method elaborated by the LESOSAI team) to determine whether the building can be labeled or not. The 80 criteria are divided in 6 areas:

- Daylight
- Noise protection
- Indoor climate
- Building design
- Materials and construction process
- Embodied energy of materials

As for embodied energy (i.e. the last point), Minergie-ECO states two limit values, the lower limit value (VL1) and the upper limit value (VL2), determining the attribution of the green mark (<VL1), orange (> VL1 and <VL2) or red (> VL2).

In contrast to the Minergie-A label, underpinning a fixed threshold value of 50 [kWh / (m^2 year)], the Minergie-ECO limit values VL1 and VL2 are variable depending on the project. As such, the Minergie-ECO label has been preferred to the Minergie-A label to assess the SolAce environmental performance.

In addition, limit values for new constructions and renovations are different. For the purposes of this report, limit values for new constructions are considered. The values VL1 and VL2 for new constructions depend on the following elements:

- Building use (housing, administration, school, etc.)
- Heated floor area
- Gross floor area
- Building renewables: geothermal boreholes, photovoltaic collectors and solar thermal collectors.

The building use determines the basic limit values $VL_{AE}1$ and $VL_{AE}2$. These are then adjusted according to the other points mentioned above to obtain the limit values VL1 and VL2. The basic limit values corresponding to the office use (i.e. administration) have been chosen for SolAce: they are equal to 30.6 [kWh / (m^2 year)] and 41.7 [kWh / (m^2 year)] respectively.

In the case of SolAce, the presence of photovoltaics and solar thermal collectors has an impact on the calculation. The Minergie-ECO methodology consists in adding to the basic limit values the embodied energy values associated to renewables production plants. As such, the limit values VL1 and VL2 amount to:

$$VL_1 = VL_{AE}1 + \frac{EE_{PV}}{HFA} + \frac{EE_{ST}}{HFA} = 30.6 + \frac{636 + 889}{94} = 46.8\ [\frac{kWh}{m^2 year}]$$

$$VL_2 = VL_{AE}2 + \frac{EE_{PV}}{HFA} + \frac{EE_{ST}}{HFA} = 41.7 + \frac{636 + 889}{94} = 57.9\ [\frac{kWh}{m^2 year}]$$

22 Discussion

The embodied energy value of SolAce is 16% lower than the VL1 proposed by the Minergie-ECO label. This demonstrates the remarkable performance of the unit in terms of embodied energy. The construction materials have a low environmental impact, and constitute a positive aspect in the SolAce energy analysis. The methodology used to calculate the embodied energy can be employed to assess the carbon emissions too, by replacing the specific embodied energy amount per reference unit with a specific emission value per reference unit. In total, the greenhouse gases emissions are illustrated in the table and charts below.

For reference, greenhouse gas emissions from a Swiss citizen amount to 4310 [kg CO_2 / year], including mobility and purchasing of goods. As shown in the summary table, the elements generating a significant fraction of the unit's embodied energy are also prominent in the calculation of greenhouse gas emissions. These are mostly the windows and the solar collectors.

Worth to note, if the unit was built using a standard concrete structure and metallic frames for windows, it would have emitted 223 [kg CO_2 / year] more, i.e. 2.3 more per heated floor area unit. Such comparison could be verified by examining an appropriate variant to the project that preserves the geometry and features a replacement of the construction elements accordingly.

Construction element	**GHG [kg CO_2 / year]**
Concrete slab	18.3
Agglomerated wood panel (OSB)	51.3
PE vapor barrier	10.3
Wood fiber insulation	80.7
Spruce tiles	10.9
3-ply panel	13.6
FERMACELL panel	20.5
Wood panel Kronotec WP50	8.3
Eurocol LiquidDesign Resin	24.1
Windows	112.1
Entrance door	4.3
PV modules	182.3
Solar thermal collectors	199.7
HVAC components	18.1
Mechanical ventilation	53.6
Sanitary equipment	14
TOTAL	**822.2**

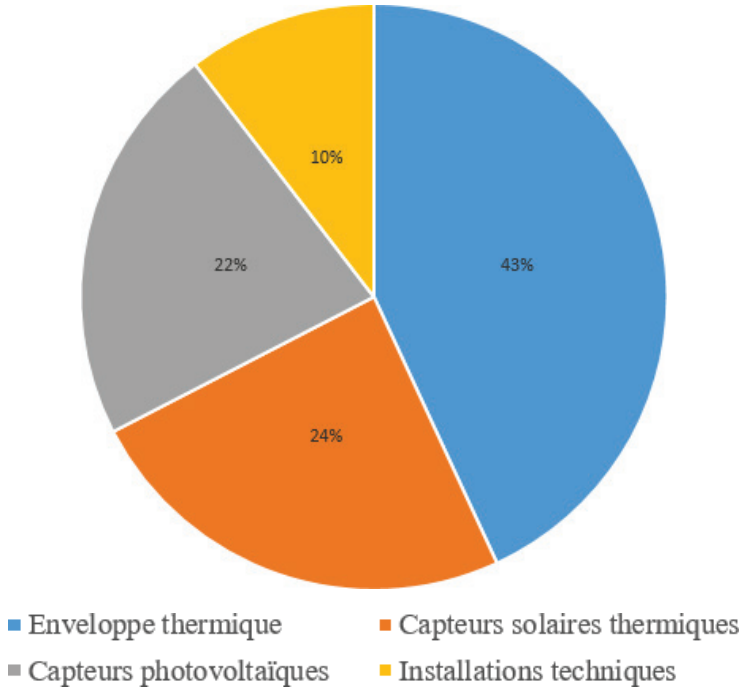

As most of the envelope constructional elements are wood products, it is worth calculating the carbon dioxide sequestration guaranteed within their lifespan. In fact, carbon stored in wood is only released back to the atmosphere when the wood product is burnt or decays. The equation used for such estimation is the following [13]:

$$m_{CO_2} = \frac{m_{dry\ wood} \cdot c \cdot f_{CO_2}}{n_{years}} = 715\ [\frac{kg_{CO_2}}{year}]$$

Where m_{CO_2} [kg] is the mass of sequestered CO_2 during the product lifespan, $m_{dry\ wood}$ [kg] is the mass of dry wood constituting the product, c [%] is the fraction of dry mass represented by carbon (considered equal to 50%), f_{CO_2} [kg/kg] is the amount of carbon dioxide cumulated in a unit of carbon mass (considered equal to 3.67 [kg/kg]). Finally, n_{years} [years] is the number of years assumed for the unit life cycle. It is worth to notice that the resulting 745 [kg CO_2 / year] are comparable with the yearly emissions quantified in 822 [kg CO_2 / year], indicating the near carbon neutrality of the unit by including the carbon sequestration of the wood products in its lifecycle.

Part VI. Conclusion

23 Overall energy balance

The overall Sankey diagram of the unit is shown in Figure 23-1. The conclusion that can be drawn from the diagram is the self-sufficiency of the unit SolAce's energy operation on a yearly basis. However, the diagram should still be interpreted as provisional, due to the following reasons:

1. On the supply side, the solar thermal production shown in the diagram implies the modification evoked in section 10, i.e. the connection of the solar thermal loop to the medium temperature network for space heating. At the present state, the solar thermal production is about half (namely 23 [kWh / (m^2 year)]. As for photovoltaic energy production, the value shown in the diagram is more consistent with monitoring.
2. On the demand side, electric appliance electricity needs (including lighting) are inferred from the current simulation and equal to 22 [kWh / (m^2 year)]; extrapolation from the monitored data features a lower value though, in the order of 17 [kWh / (m^2 year)]. If the extrapolation is sound, the photovoltaic production would be sufficient to cover the entire electricity needs on a yearly basis.
3. On the demand side, domestic hot water needs could not be determined accurately, due to the absence of a dedicated flow / energy meter. The value assumed here, is the most pessimistic between the two methodologies used for its estimation (see sections 11.1, 11.2). According to the consumer side, the domestic hot water needs could be equal to 0.7 [kWh / (m^2 year)]. The installation of a dedicated sensor is expected to solve this issue and fix the actual DHW needs.
4. On the demand side, cooling energy needs are not considered at the current stage, due to the lack of data (the first cooling season is ending at the time of writing). The cooling season is currently being analyzed by the research team. Presently, cooling needs are expected around 11 [kWh / (m^2 year)].
5. Embodied energy is not included in the diagram.

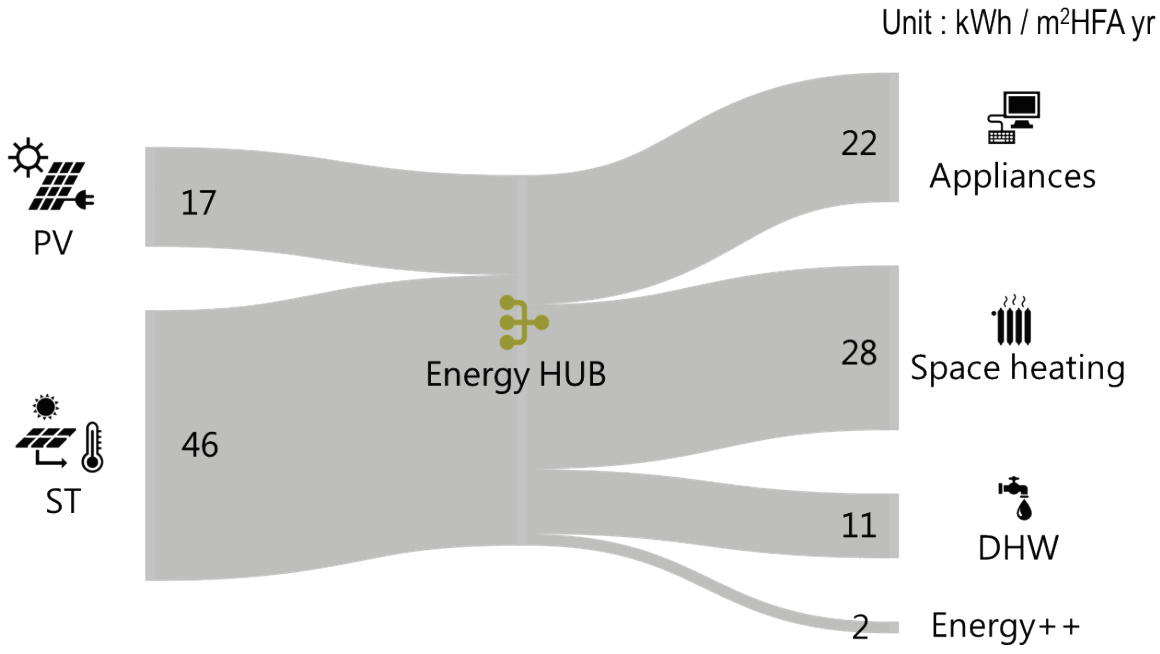

Figure 23-1 : Sankey diagram of the yearly energy needs in SolAce. The diagram does not include cooling energy needs and embodied energy.

Based on the presented results, the unit operation is already energy positive when considering space heating, domestic hot water and electric appliances needs. With the inclusion of cooling, it is reasonable to expect the energy neutrality of the unit throughout its operational phase, assuming further optimizations at the level of domestic hot water and cooling needs. Embodied energy is below the limits recommended by the label Minergie-ECO. By considering the carbon sequestration of the wood products during their lifespan, the SolAce unit can be considered also close to the carbon neutrality.

A joint research team that includes EPFL and ETHZ researchers is working to implement predictive controls for space heating and daylighting, which could further reduce the energy consumption of the SolAce unit.

References

[1] P. J. Waldram, “The Measurement of Illumination, Daylight and Artificial, with Special Reference to Ancient Light Disputes,” *J. Soc. Archit.*, vol. 3, pp. 131–140, 1909.

[2] F. O. Bartell, E. L. Dereniak, and W. L. Wolfe, “The theory and measurement of bidirectional reflectance distribution function (BRDF) and bidirectional transmittance distribution function (BTDF),” in *Radiation Scattering in Optical Systems*, 1981.

[3] M. P. Mostapha Sadeghipour Roudsari and U. S. A. Adrian Smith + Gordon Gill Architecture, Chicago, “Ladybug: a Parametric Environmental Plugin for Grasshopper To Help Designers Create an Environmentally-Conscious Design,” *13th Conf. Int. Build. Perform. Simul. Assoc.*, pp. 3129–3135, 2013.

[4] P. G. Ellis and P. a. Torcellini, “Energy Design Plugin : An EnergyPlus Plugin for SketchUp,” *Conf. Pap. NREL/CP-550-43569*, 2008.

[5] D. B. Crawley, C. O. Pedersen, L. K. Lawrie, and F. C. Winkelmann, “Energy plus: Energy simulation program,” *ASHRAE J.*, 2000.

[6] G. J. Ward, “The RADIANCE Lighting Simulation and Rendering System,” in *SIGGRAPH conference*, 1994.

[7] X. Tendon, “Modélisation et analyse énergétique d’un bâtiment sur l’ensemble de son cycle de vie - le cas de l’unité NEST-SolAce,” EPFL, 2019.

[8] “Swiss water consumption.” [Online]. Available: https://www.energie-environnement.ch/economiser-l-eau/situer-sa-consommation-d-eau. [Accessed: 12-Sep-2019].

[9] “Polysun Simulation Software,” *Velasolaris.Com*, 2012. .

[10] Conférence de coordination des services de la construction et des immeubles des maîtres d’ouvrage Publics and KBOB, “Données des écobilans dans la construction 2009/1:2016,” 2009. [Online]. Available: https://www.kbob.admin.ch/kbob/fr/home/publikationen/nachhaltiges-bauen/oekobilanzdaten_baubereich.html. [Accessed: 24-Sep-2019].

[11] S. Gerbinet, S. Belboom, and A. Léonard, “Life Cycle Analysis (LCA) of photovoltaic panels: A review,” *Renew. Sustain. Energy Rev.*, vol. 38, pp. 747–753, Oct. 2014.

[12] Minergie, “Produktreglement MINERGIE-ECO ®,” 2018. [Online]. Available: https://www.minergie.ch/media/171208_produktreglement_minergie-eco_v2018.1_de.pd.

[13] A. J. Leys, “How is carbon stored in trees and wood products?,” *Forest and Wood Products Australia*, 2012.